THE ASTROPHYSICAL JOURNAL, 277:115–131, 1984 February 1

AN X-RAY SURVEY OF A COMPLETE SAMPLE OF 3CR RADIO GALAXIES

G. FABBIANO,[1] L. MILLER,[2] G. TRINCHIERI,[1] M. LONGAIR,[3] AND M. ELVIS[1]

Received 1983 April 14; accepted 1983 July 7

ABSTRACT

We report the results of an X-ray survey with the *Einstein Observatory* of 40 3CR radio galaxies. These galaxies constitute an unbiased radio and optical sample (radio flux density >10 Jy at 178 MHz, $m_v \leq 18$, $|b| > 10°$, $\delta > 10°$). Twenty-six galaxies were detected in X-rays with (0.5–3.0 keV) X-ray luminosities between 10^{41} and 10^{45} ergs s^{-1}. By comparing the distributions of X-ray luminosities we find that 3CR galaxies with double radio morphology (FR 2) and optical emission-line spectra tend to be the more powerful X-ray emitters, with broad-line galaxies at the top of the distribution. We also find that the X-ray luminosity is strongly correlated with the 5 GHz radio nuclear luminosity. By analyzing the complete optical and radio sample with the Spearman partial rank correlation technique, we find that nuclear radio luminosity at 5 GHz is correlated with both total radio luminosity at 178 MHz and with galaxy optical luminosity. Other weaker correlations of the X-ray luminosity with the total radio luminosity at 178 MHz and the optical luminosity of the galaxy are found. These could be an effect of the radio/optical correlations reported above.

These results point to the importance of nuclear phenomena in radio galaxies and suggest a nuclear origin for their X-ray emission. Moreover, we find that the 3CR emission-line galaxies are similar to both Seyfert galaxies and quasars with double radio morphology in their X-ray properties, strongly reinforcing a unified picture of active nuclei. There is, however, a difference between double radio sources and flat spectrum quasars in the relative luminosity of their X-ray and nuclear radio emission. The non–emission-line galaxies (like 3C 264) are also likely to contain a nuclear X-ray source.

Subject headings: galaxies: nuclei — galaxies: Seyfert — quasars — radio sources: galaxies — X-rays: sources

I. INTRODUCTION

Many of the most powerful radio sources in the sky have been identified with giant elliptical galaxies. These galaxies are found in a variety of environments, in rich clusters, in groups, and in the field. Their radio structures also vary, from double-lobed sources with and without hot spots to more complex morphologies (see Miley 1980). Optically, some of these galaxies have strong emission-line spectra, similar but not identical to those of Seyfert galaxies (Osterbrock 1979). Statistical studies of a complete sample of 3CR galaxies (Jenkins, Pooley, and Riley 1977) have shown that there are correlations between the radio power and morphology and both the environment (Longair and Seldner 1979; Stocke 1979) and the presence of optical nuclear activity (Hine and Longair 1979).

There are at least three ways in which X-ray observations can provide crucial information on the astrophysics of radio galaxies, quasars, and active nuclei. First, inverse Compton scattering by the relativistic electrons responsible for the radio emission may produce intense fluxes of X-ray radiation, if the appropriate photon densities and energies of electrons are present. Second, hot gas is a necessary component of models of extended radio sources. There must be hot gas in the vicinity of the radio source to provide confinement of the radio structures. Third, there is the empirical evidence that the nuclei of radio galaxies exhibit all the properties of the most active nuclei and some are already known to be strong X-ray emitters (e.g., 3C 390.3, 3C 120, 3C 382, 3C 227; Marshall *et al.* 1978), with power law spectra similar to those of Seyfert galaxies (Petre *et al.* 1984).

The inverse Compton scattering models are probably only important either in compact nuclei where the energy densities of radiation are very great (Jones, O'Dell, and Stein 1974) or in regions of very low radio surface brightness where the inferred magnetic field strength is very low (see Harris and Grindlay 1979), $B < 10^{-6}$ gauss, such as in the most extended sources. The bremsstrahlung of the diffuse gas responsible for confining the radio components could be strong at X-ray wavelengths (see Burns, Gregory, and Holman 1981) because the characteristic densities and temperatures found from some radio source models (e.g., Hargrave and McEllin 1975) are similar to those found in rich clusters of galaxies (Schwarz *et al.* 1979). For the sources at redshifts less than 0.1 in our sample, the expected angular sizes of the X-ray sources are $\sim 3'$–$5'$ and are thus resolvable by the detectors on board the *Einstein Observatory*. Bremsstrahlung or synchrotron models can also be constructed for the X-ray emission from active nuclei (see the review by Fabian 1979).

To investigate the relative importance of these different processes for strong radio sources we have observed a complete sample of 3CR radio galaxies with the *Einstein Observatory*. An advantage of using radio galaxies rather than quasars in this analysis is that the X-ray properties of quasars appear entirely associated with processes in the active nucleus and that the optical and X-ray luminosities are strongly correlated (Tananbaum *et al.* 1979; Zamorani *et al.* 1981). This effect totally masks any of the other X-ray phenomena which might be associated with properties of the extended sources. On the

[1] Center for Astrophysics, Cambridge, Massachusetts.
[2] Mullard Radio Astronomy Observatory, Cavendish Laboratory, Cambridge, England.
[3] Royal Observatory, Edinburgh, Scotland.

other hand, in the radio galaxies, although a number contain active emission line nuclei, in many cases the nonthermal optical emission from the nucleus is weak and any X-ray emission associated with the extended radio structure should be more easily studied.

In this paper we report the results of our survey. The sample is described in § II, and the results of the observations and the data analysis are given in §§ III and IV. The distribution of X-ray luminosities and correlations with radio and optical properties are addressed in §§ V and VI. Our results are discussed in § VII.

II. THE SAMPLE

The sample includes all the 3CR sources (Jenkins, Pooley, and Riley 1977, hereafter JPR) optically identified with galaxies that satisfy the following criteria: $S \geq 10$ Jy at 178 MHz, $V \leq 18$ mag, $|b| > 10°$, and declination $> 10°$.

The source 3C 296, which was erroneously excluded from JPR, was also observed. The resulting sample contains 43 members, all with measured redshifts less than 0.2, except for 3C 109, with $z = 0.3056$. Recently, Laing, Riley, and Longair (1983, hereafter LRL) revised the JPR sample for errors due to resolution and confusion effects. If we impose a radio flux density limit of 10.8 Jy (we use here the scale of Kellerman, Pauliny-Toth, and Williams 1969), these changes would have only a very small effect upon our sample: 3C 277.3 would be excluded, and three sources should be added (DA 240, 4C 73.06, 1227+119). As we do not have X-ray data available for these extra sources, we have used the JPR sample in this paper.

LRL estimate their sample is 96% complete for sources of angular size less than 10′, so we expect to have omitted only about 1 other source. More sources with angular size greater than 10′ (e.g., DA 240, 4C 73.08) might also have been missed, but searches in the 6C survey suggest that the number is small (Baldwin 1982). Any sources which have been omitted in this way are likely to be low-luminosity sources of small redshifts. Further errors might occur owing to errors in the optical magnitudes. However, all but six sources in LRL with $18 < m_v < 19$ have photoelectric magnitudes, and we are not likely to have omitted more than one source. Hence we estimate our sample is about 94% complete for sources with angular size less than 10′ and $S \geq 10.8$ Jy and should provide an unbiased sample of strong radio galaxies.

The sample spans a wide range of radio luminosities and morphological types. At high radio luminosities ($P_{178} \gtrsim 10^{26}$ W Hz^{-1}) the majority of the sources have double morphology, and frequently show "hot spots" of high energy density towards the extremities of the source. Such sources have been classified by Fanaroff and Riley (1974) as "class 2" (hereafter FR 2). Sources with more complex morphologies tend to have lower luminosities on the average: they fail to meet the Fanaroff-Riley criterion and are classified as "class 1" (FR 1).

This sample has been thoroughly studied in other respects. The cluster membership of most of the objects has been studied by Longair and Seldner (1979), and Stocke (1979). These studies indicate that nearby ($z < 0.1$) radio sources are found in regions of higher galaxy density than is typical for galaxies in general, except that the FR 2 sources are not more likely to be found in clusters than are typical galaxies. The occurrence of optical emission lines in 3CR radio sources has been studied by Hine and Longair (1979) and Guthrie (1981): the FR 2 sources tend to have strong emission lines, whereas the FR 1 sources have less prominent emission lines.

Hine and Longair (1979) introduced a further classification based on the optical spectra: class A galaxies are those with strong emission lines and class B those with no or weak emission lines. Although in principle this classification would be a very useful one to explore the physical properties of radio galaxies, in practice it is not as well defined and reliable as the radio classification because of the uneven quality of the optical spectra available in the literature. In particular, three galaxies classified by Hine and Longair (1979) as class B galaxies—3C 277.3, 3C 285, and 3C 236—have here been reclassified as class A galaxies (Yee 1980; Miley and Osterbrock 1979).

Our sample of 43 galaxies can be subdivided in the following subsamples according to their radio or optical characteristics: (*a*) class A: 21 galaxies; (*b*) class B: 22 galaxies; (*c*) FR 1: 23 galaxies (including intermediate Fanaroff-Riley 1–2 galaxies); and (*d*) FR 2: 20 galaxies. The galaxies in the sample are listed in Table 1, with their optical and radio classifications.

Due to the demise of the *Einstein* satellite, three galaxies (3CR 35, 3CR 236, 3CR 314.1) could not be observed. Two of them are class B and one is FR 1. Since these three galaxies were not omitted because of an *a priori* choice, their exclusion should not bias our sample in any serious way.

III. X-RAY OBSERVATIONS AND DATA ANALYSIS

Forty of the 43 galaxies of the complete radio optical sample were observed with the *Einstein* satellite (Giacconi *et al.* 1979). Nineteen were observed by Center for Astrophysics either as part of this survey or in other observing programs. Three were observed as part of the present collaboration; four were observed as part of the MIT survey of radio galaxies (Feigelson and Berg 1983); six as part of the Columbia Astrophysical Laboratory survey of radio galaxies; and eight as part of other various guest observer programs. For six galaxies: 3CR 28, 3CR 83.1B, 3CR 84, 3CR 264, 3CR 272.1, and 3CR 274, we used published data or private communications from the observers (references are in Table 2). For the other galaxies, we obtained permission from the observers to analyze their data and use the X-ray fluxes for the purpose of this statistical study.

The 40 galaxies are listed in Table 2 by their 3CR number (col. [1]). Their optical positions (Smith, Spinrad, and Smith 1976) and the position of the X-ray centroid are given in columns (2) and (3). The *Einstein* sequence number, the observer, and date of the observation are given in columns (4) and (5). Most of the observations were made with the Imaging Proportional Counter (IPC). High-Resolution Imager (HRI) data are available for eight galaxies, four of which have IPC observations as well. An "I" or an "H" in front of the *Einstein* sequence number identifies the instrument.

The X-ray fluxes and luminosities were determined using the standard CFA *Einstein* software. Only counts from the Pulse Height Analyzer (PHA) channels 4–12 were used in the IPC fields to maximize the signal-to-noise ratio. In our analysis we have tried to include only flux originating from the galaxy itself. In particular we have been careful to remove extended cluster emission as far as possible. The number of source counts was derived from a circle of 120″ radius for the IPC

TABLE 1

THE COMPLETE SAMPLE

Galaxy (3CR)	Detected in X-Ray Survey	Optical Classification[a]	Radio Classification	Comments and Notes
28	X	B	1	Brightest galaxy in A115
31	X	B	1	NGC 383
33	...	A/N	2	
35	...	B	2	Not observed by *Einstein*
66B	X	B	1	In A347 (edge)
76.1	...	B	1	
83.1	...	B	1	NGC 1265 (in Perseus Cluster)
84	X	A/N	1	NGC 1275 central galaxy of A426 (Perseus Cluster)
98	X	A/N	2	
109	X	A/BL	2	
184.1	X	A/N	2	
192	X	A/N	2	
219	X	A/N	2	
223	X	A/N	2	
231	X	B	1	M82 (NGC 3034)
234	X	A/BL	2	
236	...	A/N	2	Not observed by *Einstein*
264	X	B	1	NGC 3862 in A1367
272.1	X	B	1	M84 (NGC 4374)
274	X	B	1	M87 (NGC 4486)
277.3	...	A/N	2	Reclassified as A (see Yee 1980)
285	...	A/N	2	Reclassified as A (see Yee 1980)
293	X	B	1	
296	X	B	1	NGC 5532
303	X	A	2	
305	...	A	1	
310	X	B	1	
314.1	...	B	1	Not observed by *Einstein*
315	...	A/N	1	
321	...	A/N	2	
326	...	B	2	
338	...	B	1	NGC 6166, cD in A2199
346	X	B	1	
381	...	A/BL	2	
382	X	A/BL	2	
386	X	B	1	
388	X	B	2	
390.3	X	A/BL	2	
433	X	A/N	1	
442A	...	B	1	NGC 7236
449	X	B	1	
452	...	A/N	2	
465	...	B	1	NGC 7720, cD in A2634

[a] /N are narrow emission-line galaxies; /BL are broad emission-line galaxies.

and from a circle of 18″ radius for the HRI observations. For a point source, ~85% of the counts should be contained in such cells. A correction was made to take into account the counts falling outside the cell limits in calculating the corresponding fluxes. The correction is included in the effective exposure times (col. [6]). We used different areas for 3CR 231 (M82), an extended source for which we used all the source counts, and for three more galaxies (3CR 310, 3CR 388, 3CR 449) which appear extended in the IPC. For these we used 180″ radius circles. The background was derived locally from a annulus of 400″ radius surrounding the detection circle in the IPC fields. A large box not including the source was used in the HRI fields. In the cases in which no significant source counts above the 3 σ level were detected, 3 σ upper limits were calculated. For two galaxies in clusters (3CR 338 in A2199 and 3CR 465 in A2634) no point source component could be separated from the diffuse cluster emission. For these galaxies, a 3 σ upper limit corresponding to the contribution of a point source in the cluster emission is given. This was estimated using a local background from an annulus of 15″ radius surrounding the 18″ radius source cell. The net counts with the statistical error (1 σ) or the 3 σ upper limits are also given in column (6). Column (7) lists the hydrogen column densities (N_H) from Heiles (1975) and the redshift (Smith and Spinrad 1980) for each galaxy. X-ray fluxes (in ergs cm^{-2} s^{-1}) and luminosities (in ergs s^{-1}) are given in column (8). They were calculated in a fixed energy band, between 0.5 and 3.0 keV. The derived fluxes are not sensitive to the spectral slope used. A change from $\alpha_{ph} = 1.0$ to $\alpha_{ph} = 2.0$ in the spectral index leads to variations of less than 5%. The instrumental gain variation is much more significant. The compounded uncertainty is $\pm 30\%$ in the flux (Tananbaum *et al.* 1979). We assumed a

TABLE 2

OBSERVATIONS OF 3CR RADIO GALAXIES

3CR Number (1)	R. A. (1950) Optical/X-Ray (2)	Decl. (1950) Optical/X-Ray (3)	Seq. No. (4)	Observer/Date (m/d/y) (5)	Time/Cts. Err. (6)	N_H/z (7)	(0.5–3 keV) Flux (ergs cm^{-2} s^{-1})/ L_x (ergs s^{-1}) (8)	f_x (2 keV)/ f_{RN} (5 GHz)[a,b] Jy (9)	log l_x/log l_o (ergs s^{-1} Hz^{-1}) (10)	log l_{RT}/log l_{RN} (ergs s^{-1} Hz^{-1}) (11)
28	0^{h}53^m 8^s.94	26° 8′22″.7	H10095	Gregorini[c]	...	6.1×10^{20}	1.1×10^{-12}	1.7×10^{-7}	26.53	34.51
	0 53 9.15	26 8 20.7		2/5/81	...	0.1952	1.6×10^{44}	$<1.2 \times 10^{-2}$	29.86	<31.38
31	1 4 39.18	32 8 45.8	H10566	CFA	15598	6.1×10^{20}	2.4×10^{-13}	3.8×10^{-8}	23.67	32.82
	1 4 39.14	32 8 44.0		2/14–15/81	26.3, 8.7	0.0167	2.9×10^{41}	1.4×10^{-1}	29.81	30.24
33	1 6 14.54	13 4 14.8	I3123	Tyson	2650	5.0×10^{20}	$<2.4 \times 10^{-13}$	$<3.7 \times 10^{-8}$	<24.78	33.94
				1/16/79	<22.9	0.0595	$<3.6 \times 10^{41}$	2.4×10^{-2}	29.71	30.59
66B	2 20 1.73	42 45 54.6	I3068	Maccagni	6018	1.1×10^{21}	3.4×10^{-13}	5.3×10^{-8}	24.04	32.76
	2 20 2.89	42 46 0.7		7/29/79, 8/27/79	57.0, 11.5	0.0215	6.9×10^{41}	1.6×10^{-1}	29.73	30.51
76.1	3 0 27.22	16 14 36.6	I3080	Harris	1757	1.5×10^{21}	$<2.0 \times 10^{-13}$	$<3.3 \times 10^{-8}$	<24.19	32.76
				8/2/79	<11.4	0.0324	$<9.3 \times 10^{41}$	1.0×10^{-2}	29.30	29.67
83.1B	3 14 57.00	41 40 33.4	I4478	CFA[d]	...	1.6×10^{21}	$<4.0 \times 10^{-13}$	$<6.5 \times 10^{-8}$	<23.97	32.57
				8/3–4/79	...	0.0181	$<5.8 \times 10^{41}$	2.1×10^{-2}	29.74	29.48
84	3 16 29.65	41 19 52.1	H283	CFA[e]	...	1.6×10^{21}	9.5×10^{-11}	1.3×10^{-5}	26.27	32.91
	3 16 29.70	41 19 54.0		2/2–3/79	...	0.0172	1.2×10^{44}	51.4	29.94	32.83
98	3 56 10.21	10 17 31.7	I6311	CFA	7090	1.3×10^{21}	1.0×10^{-13}	1.6×10^{-8}	23.84	33.29
	3 56 10.02	10 17 38.8		3/4/80, 8/30/80, 2/16/81	27.5, 7.8	0.0306	4.2×10^{41}	9.0×10^{-3}	29.42	29.57
109	4 10 54.82	11 4 41.2	I1935, I1936	CAL	1856	1.3×10^{21}	2.0×10^{-12}	3.2×10^{-7}	27.23	35.06
	4 10 54.66	11 5 15.3		3/7/79, 8/13/79	156.5, 13.0	0.3056	1.0×10^{45}	1.9×10^{-1}	30.11	33.00
184.1	7 34 28.20	80 33 32.0	I7719	Longair	5485	6.1×10^{20}	1.3×10^{-13}	2.2×10^{-8}	25.16	33.94
	7 34 50.45	80 33 34.8		3/5–6/80	30.3, 8.2	0.1182	8.8×10^{42}	8.0×10^{-3}	29.61	30.61
192	8 2 35.51	24 18 28.2	I6322	CFA	4469	5.0×10^{20}	1.1×10^{-13}	1.7×10^{-8}	24.45	33.54
	8 2 39.26	24 19 48.9		4/6/80	19.4, 6.7	0.0599	1.8×10^{42}	8.0×10^{-3}	29.61	30.11
219	9 17 50.66	45 51 43.9	I6315	CFA	747	2.3×10^{20}	1.5×10^{-12}	2.5×10^{-7}	26.59	34.81
	9 17 52.58	45 52 20.7		4/24/80	53.9, 7.8	0.1744	2.4×10^{44}	4.2×10^{-2}	29.88	31.81
223	9 36 50.91	36 7 34.9	I7720	Longair	4138	1.7×10^{20}	1.2×10^{-13}	2.0×10^{-8}	25.26	34.13
	9 36 51.80	36 8 3.0		5/15–16/80	23.3, 7.1	0.1368	1.1×10^{43}	8.5×10^{-3}	29.72	30.90
231	9 51 42.70	69 54 59.0	H586	CFA	13110	5.0×10^{20}	1.3×10^{-11}	2.2×10^{-6}	22.89	29.71
				5/3–6/80	1307.6, 45.0	0.0009	4.6×10^{40}	1.8×10^{-1}	28.77	27.80
234	9 58 57.42	29 1 37.4	I2687	MIT	1478	2.8×10^{20}	2.5×10^{-13}	4.0×10^{-8}	25.85	34.74
	9 58 55.42	29 2 3.8		5/24/79	17.6, 5.1	0.1848	4.3×10^{43}	9.0×10^{-2}	29.91	32.20
264	11 42 29.64	19 53 2.5	I296	CFA[f]	...	1.0×10^{21}	1.2×10^{-12}	2.0×10^{-7}	24.59	32.69
	11 42 29.90	19 53 7.0		12/18/78, 12/18–19/79	...	0.0208	2.3×10^{42}	2.5×10^{-1}	29.76	30.68
272.1	12 22 32.47	13 9 54.8	I4320	CFA[g]	...	4.0×10^{20}	5.4×10^{-13}	9.0×10^{-8}	22.58	30.91
				6/22/80	...	0.0031	2.6×10^{40}	1.8×10^{-1}	29.44	28.87
274	12 28 17.60	12 40 2.0	H282	CFA[h]	...	2.8×10^{20}	2.1×10^{-12}	3.4×10^{-7}	23.44	32.92
				7/6–10/79	...	0.0043	1.7×10^{41}	4.0	29.99	30.51
277.3	12 51 46.29	27 53 49.5	I3917	Silk	2540	2.8×10^{20}	$<2.4 \times 10^{-13}$	$<3.9 \times 10^{-8}$	<25.13	33.63
				7/3/79	<28.2	0.0857	$<8.1 \times 10^{42}$	1.6×10^{-2}	29.74	30.74
285	13 19 5.10	42 50 47.1	I3120	Tyson	5415	1.7×10^{20}	$<1.5 \times 10^{-13}$	$<2.6 \times 10^{-8}$	<24.88	33.53
				12/8/79, 1/8/80	<35.8	0.0794	$<4.4 \times 10^{42}$	6.0×10^{-3}	29.65	30.25
293	13 50 3.44	31 41 32.2	I6327	CFA	3714	1.7×10^{20}	1.7×10^{-13}	2.7×10^{-8}	24.40	33.07
	13 50 4.75	31 41 7.5		6/19/80	25.1, 6.7	0.0452	1.5×10^{42}	<1.6	29.81	<32.17
296	14 14 26.96	11 2 15.1	I1905	CAL	3856	1.7×10^{20}	2.5×10^{-13}	4.0×10^{-8}	24.00	32.51
	14 14 24.01	11 1 30.2		1/24/79	34.9, 8.3	0.0237	6.1×10^{41}	7.7×10^{-2}	30.09	30.28
303	14 41 24.84	52 14 18.7	I6317	Longair	5373	1.7×10^{20}	1.2×10^{-12}	2.0×10^{-7}	26.29	34.04
	14 41 27.28	52 14 24.9		6/2/80	316.3, 19.3	0.1410	1.2×10^{44}	1.5×10^{-1}	29.73	32.17
305	14 48 17.58	63 28 36.4	I6318	CFA	4260	1.7×10^{20}	$<1.7 \times 10^{-13}$	$<2.7 \times 10^{-8}$	<24.32	33.07
				7/23/80	<30.6	0.0410	$<1.3 \times 10^{42}$	$<2.0 \times 10^{-1}$	29.96	<31.18
310	15 2 47.50	26 12 30.0	I1907	CAL[i]	8682	5.0×10^{20}	8.3×10^{-13}	1.4×10^{-7}	25.26	33.87
	15 2 47.18	26 12 32.4		8/12–13/80	263.4, 20.5	0.0540	1.1×10^{43}	8.9×10^{-2}	29.60	31.07

TABLE 2—*Continued*

3CR Number (1)	R. A. (1950) Optical/X-Ray (2)	Decl. (1950) Optical/X-Ray (3)	Seq. No. (4)	Observer/Date (m/d/y) (5)	Time/Cts. Err. (6)	N_H/z (7)	(0.5–3 keV) Flux (ergs cm^{-2} s^{-1})/ L_x (ergs s^{-1}) (8)	f_x (2 keV)[a, b] f_{RN} (5 GHz)[b, i] Jy (9)	log l_x/log l_o (ergs s^{-1} Hz^{-1}) (10)	log l_{RT}/log l_{RN} (ergs s^{-1} Hz^{-1}) (11)
315	15 11 30.80	26 18 35.0	I1909	CAL	2562	3.9×10^{20}	$<3.0 \times 10^{-13}$	$<4.2 \times 10^{-8}$	<25.37	34.03
				1/29/79, 8/13/80	<27.0	0.1083	$<4.3 \times 10^{43}$	1.5×10^{-1}	29.61	31.93
321	15 29 33.44	24 14 26.5	I3121	Tyson	2857	5.6×10^{20}	$<2.9 \times 10^{-13}$	$<4.8 \times 10^{-8}$	<25.32	33.77
				7/20/79	<35.6	0.0960	$<1.3 \times 10^{43}$	3.0×10^{-2}	29.82	31.12
326	15 50 14.00	20 16	I371	CFA	4414	5.0×10^{20}	$<1.0 \times 10^{-13}$	$<9.3 \times 10^{-9}$	<24.55	33.66
				8/11/80	<17.7	0.0895	$<3.9 \times 10^{42}$	1.3×10^{-2}	29.36	30.69
338	16 26 55.38	39 39 36.6	H379, H380	CFA	8218	1.7×10^{20}	$<1.3 \times 10^{-12}$	$<2.1 \times 10^{-7}$	<24.94	33.28
				7/11/79, 8/23/79	<102.0	0.0303	$<5.3 \times 10^{42}$	1.5×10^{-1}	30.14	30.78
346	16 41 34.71	17 21 19.7	I6328	CFA	2893	6.7×10^{20}	1.1×10^{-12}	1.8×10^{-7}	26.36	34.15
	16 41 33.98	17 20 55.3		3/9/80	136.0, 12.7	0.1610	1.4×10^{44}	2.2×10^{-1}	29.90	32.45
381	18 32 14.43	47 24 39.0	I426	CFA	3530	6.1×10^{20}	$<1.4 \times 10^{-13}$	$<2.3 \times 10^{-8}$	<25.47	34.33
				10/8/79	<21.0	0.1605	$<1.8 \times 10^{43}$	5.2×10^{-3}	29.79	30.83
382	18 33 12.11	32 39 15.1	I2650	MIT	1006	1.1×10^{21}	1.3×10^{-11}	2.2×10^{-6}	26.53	33.48
	18 33 11.33	32 38 43.0		3/27/79	503.4, 22.8	0.0578	2.0×10^{44}	1.7×10^{-1}	29.90	31.41
386	18 36 12.87	17 9 6.9	I6329	CFA	8520	3.0×10^{21}	1.8×10^{-13}	3.0×10^{-8}	23.58	32.48
	18 36 13.70	17 8 39.6		3/20, 3/22/80	50.0, 11.5	0.0170	2.3×10^{41}	1.4×10^{-2}	28.68	29.25
388	18 42 35.44	45 30 21.7	I2693	MIT	1702	6.1×10^{20}	1.9×10^{-12}	2.8×10^{-7}	26.04	33.98
	18 42 36.40	45 30 39.1		10/30/79	113.8, 12.5	0.0908	6.6×10^{43}	6.2×10^{-2}	30.04	31.38
390.3	18 45 37.80	79 43 3.4	H342	CFA	2002	5.6×10^{20}	1.8×10^{-11}	3.0×10^{-6}	26.64	33.85
	18 45 37.60	79 43 5.9(+10″)		11/21/78	276.5, 16.9	0.0569	2.6×10^{44}	3.4×10^{-1}	29.84	31.70
433	21 21 30.50	24 51 33.0	I5712	CAL	8975	8.4×10^{20}	9.0×10^{-14}	1.5×10^{-8}	24.86	34.44
	21 21 30.03	24 51 45.0		11/19–20/79	32.4, 10.2	0.1016	4.4×10^{42}	$<2.5 \times 10^{-2}$	29.77	<31.09
442	22 12 19.50	13 35 41.0	H1913	CAL	4526	6.1×10^{20}	$<5.0 \times 10^{-13}$	$<8.0 \times 10^{-8}$	<24.39	32.72
				5/31/79	<16.2	0.0263	$<1.6 \times 10^{42}$	1.9×10^{-3}	29.60	28.76
449	22 29 7.71	39 6 4.4	I3916	Silk	1914	1.2×10^{21}	9.8×10^{-13}	1.6×10^{-7}	24.31	32.17
	22 29 7.35	39 6 8.9		6/11/80	63.1, 7.8	0.0171	1.2×10^{42}	3.7×10^{-2}	29.41	29.68
452	22 43 33.00	39 25 25.6	I2681	MIT	1452	1.2×10^{21}	$<4.8 \times 10^{-13}$	$<7.8 \times 10^{-8}$	<25.38	34.22
				1/8/80	<26.4	0.0811	$<1.5 \times 10^{43}$	1.3×10^{-1}	29.66	31.60
465	23 35 59.00	26 45 18.0	H10192	CFA	26310	6.1×10^{20}	$<2.4 \times 10^{-13}$	$<3.9 \times 10^{-1}$	<24.17	33.16
				12/25–27/80	<45.6	0.0293	$<8.9 \times 10^{41}$	2.7×10^{-1}	29.84	31.01

[a] The f_{RN} (5 GHz) for the three galaxies not observed in X-rays are: 1.4×10^{-2} (3CR 35), 4.0×10^{-1} (3CR 236), and $<1.0 \times 10^{-2}$ (3CR 314.1).

[b] The references for the 5 GHz radio nuclear flux densities are as follows: 3CR 28 (J. T. Macklin 1982, private communication); 3CR 31 (JPR); 3CR 33 (Hargrave and McEllin 1975); 3CR 35 (Van Breugel 1980*a*); 3CR 66B (P. Leahy and G. G. Pooley 1982, private communications); 3CR 76.1 (Macklin 1983); 3CR 83.1B (Riley and Pooley 1975; Owen, Burns, and Rudnick 1978); 3CR 84 (Elsmore and Ryle 1976); 3CR 98 (Fomalont and Bridle 1978); 3CR 109 (Hine and Scheuer 1980); 3CR 184.1 (Riley and Pooley 1975); 3CR 192 (Högbom 1979); 3CR 219 (Perley *et al.* 1980); 3CR 223 (Riley and Pooley 1975; Van Breugel 1980*a*); 3CR 231 (Hargrave 1974); 3CR 234 (Riley and Pooley 1975); 3CR 236 (Fomalont, Bridle, and Miley 1982); 3CR 264 (Bridle and Vallée 1981 and references therein); 3CR 272.1 (R. A. Laing 1982, private communication); 3CR 274 (Turland 1975); 3CR 277.3 (Bridle *et al.* 1981*a*); 3CR 285 (R. A. Laing 1982, private communication); 3CR 293 (Argue *et al.* 1978; Bridle *et al.* 1981*b*); 3CR 296 (Fomalont, Palimaka, and Bridle 1980); 3CR 303 (Pooley and Henbest 1974); 3CR 305 (Heckman *et al.* 1982); 3CR 310 (Van Breugel 1980*b*); 3CR 314.1 (Cambridge 5 km telescope data, unpublished); 3CR 315 (Högbom 1979); 3CR 321 (JPR); 3CR 326 (Willis and Strom 1978); 3CR 338 (JPR); 3CR 346 (D. Stannard 1982, private communication); 3CR 381 (Miller and Laing 1983); 3CR 382 (Strom, Willis, and Wilson 1978); 3CR 386 (Strom, Willis, and Wilson 1978); 3CR 388 (Burns and Christiansen 1980); 3CR 390.3 (van Breugel 1980*a*); 3CR 433 (Pooley and Henbest 1974); 3CR 442 (R. A. Laing 1982, private communication); 3CR 449 (Perley, Willis, and Scott 1979); 3CR 452 (Riley and Pooley 1975); 3CR 465 (P. Leahy and G. G. Pooley 1982, private communication).

[c] Gregorini *et al.* 1983.

[d] Fabricant *et al.* 1979.

[e] Branduardi-Raymont *et al.* 1981.

[f] Elvis *et al.* 1981.

[g] Forman *et al.* 1979.

[h] Schreier, Gorenstein, and Feigelson 1982.

[i] Also observed by Burns, Gregory, and Holman 1981. They find consistent results.

power-law spectrum with a photon index $\alpha_{ph} = 1.0$. In deriving the X-ray fluxes, a correction for galactic interstellar absorption was applied using the N_H in column (7). The intrinsic absorption at the source is unknown. The effect of intrinsic absorption on the detected X-ray flux is discussed in §§ VII*b* and VII*c*. A Hubble constant of 50 km s^{-1} Mpc^{-1} and $q_0 = 0$ have been used throughout. Column (9) lists the monochromatic X-ray flux density at 2 keV and the radio nuclear flux density at 5 GHz. Both quantities are in Janskys. Columns (10) and (11) list the log of the monochromatic X-ray, optical, and radio luminosities. l_{RT} is the total monochromatic radio luminosity at 178 MHz; l_{RN} is the monochromatic nuclear radio luminosity at 5 GHz; these quantities are in units of ergs s^{-1} Hz^{-1}.

IV. X-RAY RESULTS AND COMMENTS ON INDIVIDUAL SOURCES

Twenty-six of the 40 galaxies observed with the *Einstein Observatory* were detected at least at the 3 σ level. They are divided between the optical and radio classes as follows: 12 in class A, 14 in class B, 15 in class FR 1, and 11 in class FR 2. The (0.5–3.0 keV) X-ray fluxes range from 0.9×10^{-13} to 1.9×10^{-11} ergs cm^{-2} s^{-1}. The (0.5–3.0 keV) X-ray luminosities range from 1.7×10^{41} to 1.0×10^{45} ergs s^{-1}. The fluxes and luminosities for 3CR 66B and 3CR 338 listed in Table 2 are smaller than those given by Feigelson and Berg (1983) (of a factor of 2.4 for 3CR 66B and >12 for 3CR 338). The different cell sizes used to determine the source counts (4′ in their paper) and the angular extent of the X-ray emission (see the next section) explain the discrepancy.

Twenty-one of the 26 sources detected and listed in Table 2 were available to us for analysis. Comparing the positions of the X-ray centroids with those of the optical galaxies (Smith, Spinrad, and Smith 1976), we found angular separations $\leq 0.'5$ for 14 galaxies and between $0.'5$ and $1.'0$ for six, compatible with the positional uncertainty of our IPC data (1′). Only for 3CR 192 did we find an angular separation larger than 1′. This is likely to be due to the presence of a background blue object (see below). The HRI sources are all within 3″ of the optical positions, compatible with the HRI positional uncertainty. Given the size of our sample, the 3 σ threshold chosen and the positional coincidences, we are confident of the association of the X-ray emission with these 3CR galaxies.

Table 3 summarizes the information on the angular extent of the X-ray sources. Since most of the galaxies were observed with the IPC we cannot generally distinguish between nuclear emission or an emission region the size of the whole galaxy on the basis of the X-ray images alone. For at least one of the galaxies, 3CR 264, the HRI image gives a size <1 kpc, consistent with a nuclear source. This galaxy does not display any sign of an active nucleus in its optical spectrum (Elvis *et al.* 1981). Also, 3CR 390.3 is pointlike in the HRI. This galaxy has an emission-line nucleus. A nuclear component is also present together with an extended halo in M87 (3CR 274) (Schreier, Gorenstein, and Feigelson 1982) and NGC 1275 (3CR 84) (Branduardi-Raymont *et al.* 1981).

Some of the galaxies in our sample are associated with regions of extended X-ray emission. Besides 3CR 84 (NGC 1275) in the Perseus Cluster (Branduardi-Raymont *et al.* 1981) and 3CR 272.1 and 3CR 274 (M84 and M87) in Virgo (Forman *et al.* 1979) where extended X-ray halos are present, 3CR 66B (Maccagni and Tarenghi 1981) and 3CR 310 (Burns, Gregory, and Holman 1981) have also been reported as extended. The galaxy 3C 231 (M82), observed with the HRI, appears extended on a scale of 20″ (Watson and Griffiths 1980), but this emission is entirely within the optical galaxy and is therefore presumably different from the extended cluster emission that is present in most of the other cases. The presence of an extended X-ray source associated with 3CR 449 could be due to the associated cluster (Miley *et al.* 1983). We find that 3CR 31 and 3CR 338 are also associated with regions of extended X-ray emission. These two galaxies are both in regions of high galaxy density and will be discussed in detail in a future paper.

TABLE 3

ANGULAR EXTENT OF THE X-RAY EMISSION

Galaxy (3CR)	Extent (arcmin)
28	~0.3
31	Extended cluster emission
66B	Extended (Maccagni and Tarenghi 1981)
84	Extended cluster emission and nuclear component (Branduardi-Raymont *et al.* 1981)
98	Too few counts detected
109	Data not available for extent analysis
184.1	<15.0
192	$0.8^{+1.7}_{-0.3}$ (>0.2)
219	<10.7
223	Too few counts detected
231	0.3 (Watson and Griffiths 1980)
234	Too few counts detected
264	Pointlike ($\lesssim 3''$) (Elvis *et al.* 1981)
272.1	Extended ~3′ core-radius (Forman *et al.* 1979)
274	Nuclear component and extended halo (Forman *et al.* 1979; Schreier, Gorenstein, and Feigelson 1982)
293	$1.2^{+1.3}_{-0.4}$ (>0.6)
296	Data not available for extent analysis
303	<0.6
310	1.5 + 0.2 (Burns, Gregory, and Holman 1981)
338	Extended cluster emission
346	<1.2
382	<0.3
386	<13.0
388	$0.8^{+0.2}_{-0.1}$ (>0.6)
390.3	Pointlike ($\lesssim 3''$)
433	Data not available for extent analysis
449	$1.2^{+0.2}_{-0.3}$ (>0.7) (Miley *et al.* 1983)

We investigated the angular extent of 10 IPC sources not obviously located inside a rich cluster assuming a Gaussian X-ray surface brightness distribution and calculating the Gaussian σ from the ratio of the counts in an inner circle of radius 1.'3 to those in the surrounding annulus of the same radius (Henry *et al.* 1979). To derive the Gaussian standard deviations we used PHA channels ≥ 4. Applying the same analysis to a point source (3C 273) we obtained the IPC point response function (see also Fabbiano, Feigelson, and Zamorani 1982). In Table 3 we give the best fit values together with the 68% errors for the galaxies for which extent was detected at better than 99.7% confidence. The 99.7% lower limits are given in parentheses. Otherwise we give the 99.7% upper limits to the extent. The galaxies 3CR 192, 3CR 293, and 3C 388 appear extended at better than the 99.7% level. In 3CR 192 and 3CR 293, the extension could be due to chance superposition with a background object. In the case of 3CR 192 (which is also the galaxy with the largest discrepancy between the X-ray and radio positions), a ~20.5 mag blue

object is just visible at the X-ray centroid in the Palomar Observatory Sky Survey O plate. If this object is a background QSO, we would expect an X-ray flux similar to that detected on the basis of the mean optical to X-ray ratios of quasars (Zamorani *et al.* 1981). Moreover the distribution of counts is asymmetric and consistent with two nearby sources of comparable intensity, one located on the radio galaxy and one on the QSO.

The galaxy 3CR 293 appears projected onto the background Zwicky cluster Zw 1350.0+3148 ($z = 0.14$; Stocke 1979). Since the X-ray luminosity of clusters is in the range of 10^{43}–10^{44} ergs s^{-1} (McKee *et al.* 1980), a cluster at a redshift $z = 0.14$ could be detectable with a flux comparable to or higher than that of 3CR 293. Moreover the optical size of the cluster from the Zwicky catalog is consistent with the size derived from the IPC image. We therefore suspect a contamination with this background object. We shall take the fluxes of 3CR 192 and 3CR 293 to be as derived in the standard way but will bear in mind the above problems when we analyze the correlations.

The galaxy 3CR 382 has an upper limit to its extent smaller than the extent of the radio lobes ($\sim 2'$) and 3CR 303 comparable to the radio extent. For the other IPC sources the statistics were not good enough to give meaningful upper limits.

V. THE DISTRIBUTION OF THE X-RAY LUMINOSITY

The histograms of the X-ray luminosity, L_x, for the total sample, for the two radio subsamples FR 1 and FR 2, and for the optical subsamples A and B are shown in Figures 1*a*–1*c*. Both detections and upper limits indicated by open and hatched boxes, respectively, are plotted. The broad-line galaxies are indicated by "BL" in the plots.

Not surprisingly, the distributions of L_x for FR 1 and FR 2 galaxies are essentially the same as those for class B and class A, respectively. Since FR 1 $\cong$ class B and FR 2 $\cong$ class A and since moreover the optical classification is somewhat uncertain (see § II), in what follows we will refer mainly to the radio classification.

We notice that the FR 2 subsample tends to include higher luminosity galaxies than the FR 1. The FR 1 galaxies are also biased toward higher luminosities by cluster emission, as we discuss in a moment, so that the difference should be in reality even more pronounced. Moreover the galaxies with broad permitted lines in their spectra are among those with the highest luminosities ($L_x > 10^{43}$–10^{45} ergs s^{-1}).

In the previous paragraph we have simply made a straight comparison between the luminosities of FR 1 and FR 2 galaxies, without considering possible biases in the X-ray fluxes. In fact, an obvious bias in the determination of the X-ray fluxes is due to the presence of cluster emission in the field of some of the 3CR galaxies. Clusters of galaxies are strong diffuse X-ray sources (e.g., Forman and Jones 1982). Since most observations were made with the IPC, which has an angular resolution of $\sim 0'.9$ FWHM, a significant amount of cluster emission could be included in our estimate of the X-ray flux, especially for the more distant galaxies. This is especially true when the radio galaxy is the dominant galaxy of a cluster and is near the center of the cluster. To estimate how much our results are affected by the presence of X-ray emitting cluster medium or extended halos, like the one around NGC 1275 (Branduardi-Raymont *et al.* 1981), we performed the following experiment.

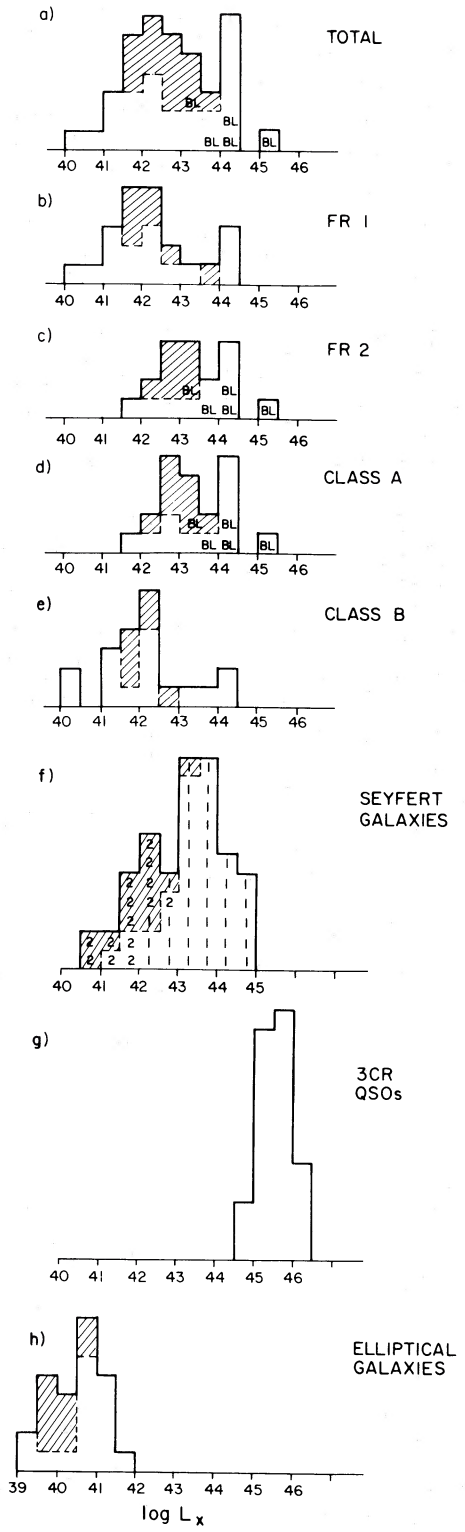

FIG. 1.—Histograms of L_x for (*a*), the total observed sample of 40 3CR galaxies; (*b*) and (*c*) the FR 1 and FR 2 radio subsamples; (*d*) and (*e*) the class A and class B optical subsamples; (*f*) Seyfert galaxies; (*g*) 3CR quasars; and (*h*) elliptical galaxies.

We calculated the *linear* dimension corresponding to the 2′ radius of the IPC detection circle for the second most distant galaxy in our sample (523 kpc, 3CR 28) and used detection cells with angular radii corresponding to the same linear dimension for all the galaxies in the sample. We did not use the most distant galaxy (3CR 109) because it is at a considerably higher redshift than the rest of the sample. The effect on the "galaxy" luminosities is shown in Figure 2. Here we plot the histograms of L_x for FR 1 and FR 2 galaxies using the fluxes in the table (same angular cell) (Figs. 2*a* and 2*b*) and the fluxes derived from detection cells corresponding to the same linear dimension in the sky as explained above (Figs. 2*c* and 2*d*). As can be seen from the figure, the distributions of L_x for FR 2 galaxies (typically not in clusters) are the same in the two cases. In fact point-by-point comparison shows no excess flux from the surrounding areas. In contrast the distribution of L_x for FR 1 galaxies has moved toward higher luminosities, due to the inclusion of extra cluster emission when the detection cells corresponding to the same linear dimensions are used.

The effect of the removal of this bias from the distribution of L_x for FR 1 galaxies (Fig. 1) would result in a shift toward lower luminosities, especially at the higher luminosity end, and would move the distribution of the X-ray luminosities of the two classes further apart. Of course, the presence of diffuse emission around the radio galaxies in clusters and the absence of the same from the regions surrounding isolated FR 2 galaxies (see § IV), have implications for the problem of the confinement of the extended radio structures. This will be the subject of a future paper (Miller *et al.* 1984, hereafter Paper II).

In Figure 1 we also plot for comparison the histograms of the X-ray luminosities of Seyfert galaxies (from Kriss, Canizares, and Ricker 1980), 3CR quasars (Tananbaum *et al.* 1983), and normal elliptical galaxies (from the review of Long and Van Speybroeck 1982). The X-ray luminosities of Seyfert galaxies are distributed similarly to those of the total 3CR radio galaxy sample, with Seyfert type 1 galaxies being comparable with the luminous broad-line radio galaxies. The X-ray luminosities of the 3CR quasars are higher. The distribution of L_x of normal elliptical galaxies could be compatible with the

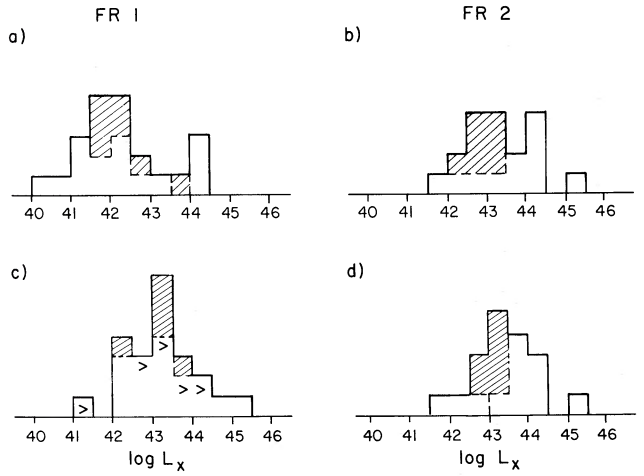

FIG. 2.—Histograms of L_x for FR 1 and FR 2 galaxies using the fluxes from Table 2 [(*a*) and (*b*)] and using detection cells corresponding to the same linear dimension (see text) [(*c*) and (*d*)].

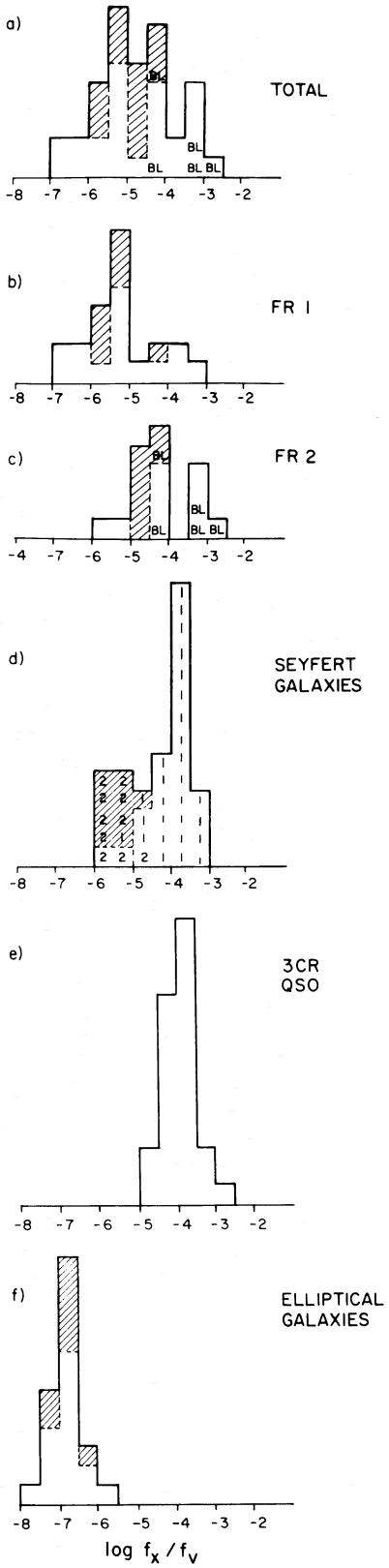

FIG. 3.—Histograms of f_x/f_o for (*a*) the total observed sample of 40 3CR galaxies; (*b*) and (*c*) the FR 1 and FR 2 radio subsamples; (*d*) Seyfert galaxies; (*e*) 3CR quasars; and (*f*) elliptical galaxies.

less luminous of the FR 1 3CR galaxies, but is definitely below that of the FR 2 galaxies.

Figures 3*a*–3*f* show the histograms of the X-ray to the integrated optical (f_x/f_o) flux ratio (where the fluxes are the monochromatic fluxes at 2 keV and in the V band) for the 3CR galaxies and the other objects shown in Figure 2. The ratio f_x/f_o covers a broad range. The broad-line galaxies have ratios at the high end of the distribution, which are similar to those of Seyfert 1 galaxies and 3CR quasars. This is reasonable if the X-ray and optical emission in these radio galaxies is dominated by nuclear nonthermal radiation.

For narrow-line and FR 1 galaxies f_o is dominated by the stellar light of the parent elliptical galaxy. The absolute magnitude of these galaxies is much larger than the typical values for Seyfert galaxies. At the low end of the distribution some FR 1 galaxies have f_x/f_o ratios similar to those of normal ellipticals.

VI. CORRELATIONS BETWEEN RADIO, OPTICAL, AND X-RAY PROPERTIES

Before investigating the relationship between X-ray and other properties, we shall explore the relationship between the radio and optical properties of the sample. Nuclear radio fluxes are available (see Table 2), for 38 of the 43 galaxies of the complete radio and optical sample and upper limits for five. In FR 2 galaxies the cores usually have flat spectra (Laing 1981*b*) and are thought to consist of compact components which are self-absorbed at 6 cm. This is borne out by VLBI observations (Schilizzi 1976; Preuss *et al.* 1977; Pearson and Readhead 1981). Only one of the FR 2 sources (3C 236) is known to have a steep-spectrum, extended core (Fomalont, Bridle, and Miley 1982). This source is also known to have a compact core, however, although its flux density is rather uncertain. In the FR 1 sources, however, the situation is different. Many FR 1 sources have luminous jets extending into the core, and the core fluxes derived from 2″ resolution maps may be seriously overestimated. Where available, we have used higher resolution VLA observations to help eliminate this problem, but contamination of the radio core fluxes may still occur. Similarly, as discussed in the previous section, for galaxies in clusters (FR 1) the X-ray flux could be an overestimate of the flux from the galaxy itself. The FR 2 galaxies should not suffer from observational (instrumental) biases in either the radio or the X-rays. Bearing this in mind we have looked for relationships between optical, radio, and X-ray properties.

a) Correlations between the Optical Luminosities and the Luminosities of the Radio Cores and Lobes

Figures 4*a*, 4*b*, and 4*c* show plots of the radio nuclear 5 GHz luminosity l_{RN} versus the total radio luminosity at 178 MHz l_{RT}; of l_{RN} versus the V band monochromatic luminosity of the galaxies l_o; and of l_{RT} versus l_o for the total complete sample of 43 galaxies and for FR 1 and FR 2 galaxies, respectively. The plots for FR 1 galaxies show more scatter than those for FR 2 galaxies. In all plots correlations are apparent.

In Table 4 we give the correlation coefficient (SR) and probability (P_{SR}), that the given correlation might arise by chance, calculated with the nonparametric Spearman rank correlation test (Kendall and Stuart 1976). All correlations appear significant. To calculate P_{SR} we ignored the five upper limits in l_{RN}. Inclusion of these limits with the worst possible ranking results in nonsignificant correlations between l_{RN} and both l_{RT}, l_o for FR 1 galaxies. Applying a linear regression method, we calculated the slopes of each correlation. These slopes are also given in Table 4 along with their statistical (1 σ) errors. Inclusion of the upper limits with an application of the "detection and bounds" method (Avni *et al.* 1980; Avni 1984; see also next section) gives consistent and significant results in all cases.

In interpreting the correlations we must take into account strong selection effects, mainly of a dependence on the redshift z resulting from the flux limits in the optical and radio 178 MHz fluxes. The parameter l_{RN} is not *a priori* biased, so at least one

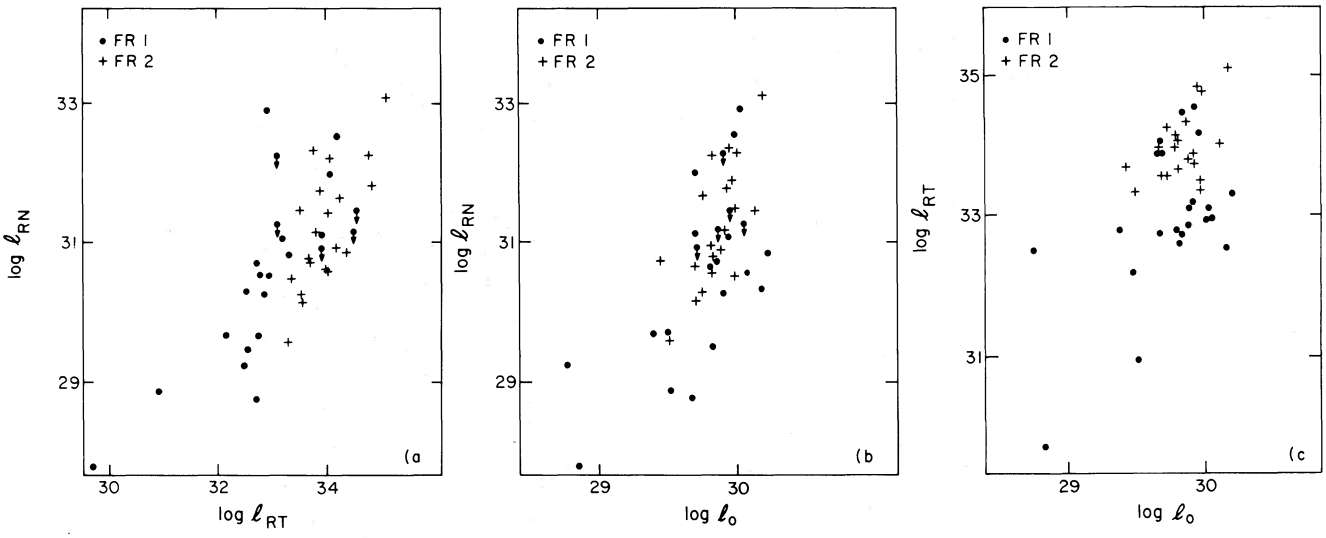

FIG. 4.—(*a*) The logarithm of the nuclear radio power l_{RN} is plotted vs. the logarithm of the 178 MHz total radio power; (*b*) log l_{RN} is plotted vs. the logarithm of the optical luminosity l_o; (*c*) log l_{RT} is plotted vs. log l_o.

TABLE 4

SR CORRELATION PROBABILITIES (ONE-TAILED) AND LINEAR FIT SLOPES FOR RADIO AND OPTICAL LUMINOSITIES

	TOTAL			FR 1			FR 2		
$y \propto x$	SR	P_{SR}	Slope	SR	P_{SR}	Slope	SR	P_{SR}	Slope
$l_{RN} \propto l_o$.....	0.59	<0.05%	2.75 ± 0.40[a]	0.62	<1%	2.15 ± 0.45[a]	0.67	<1%	...
			2.38 ± 0.46[b]			2.01 ± 0.62[b]			3.03 ± 0.77[b]
$l_{RN} \propto l_{RT}$.....	0.76	<0.05%	0.75 ± 0.05[a]	0.83	<1%	0.75 ± 0.10[a]	0.66	<1%	...
			0.89 ± 0.12[b]			0.98 ± 0.19[b]			1.24 ± 0.29[b]
$l_{RT} \propto l_o$.....	0.28	4%	1.74 ± 0.43[b]	0.47	3%	1.58 ± 0.53[b]	0.34	5%	1.30 ± 0.52[b]

[a] With the "detections and bounds" method.
[b] Linear regression, ignoring the upper limits.

of the correlations between l_{RN} and l_{RT} or l_{RN} and l_o is real. We are not able however to state immediately which of the correlations between l_{RN}, l_{RT}, l_o is fundamental.

We investigated this problem using a Spearman partial rank correlation test (Kendall and Stuart 1976), a method widely used in the behavioral and biological sciences (see Siegel 1956) to analyze a many variable problem and disentangle the real correlations from those introduced by the relationship between the variables (see also Macklin 1982 and Tananbaum *et al.* 1983 for applications in astrophysics). We applied this method to a three-variable case, including simultaneously l_o, l_{RT}, and l_{RN} and ignoring the upper limits. The partial correlation coefficients (ON.T, OT.N, and NT.O) and the corresponding probabilities, obtained from the Student t-distribution, are shown in Table 5 for the total sample and for the FR 1 and FR 2 radio subsamples separately.

Large correlation coefficients (and correspondingly small probabilities that the correlation might arise by chance) are obtained in all samples for the correlations of l_{RN} with both l_{RT} and l_o for fixed values of the variable not involved. The total radio power at 178 MHz l_{RT} and the optical luminosity l_o are not correlated in the FR 1 and FR 2 subsample and are, if anything, anticorrelated in the total sample. These two variables are both flux limited and therefore likely to show a correlation arising from both being correlated with the redshift z (a selection effect). Therefore the lack of a positive correlation between these two variables, when considered simultaneously with l_{RN} shows that the nuclear radio power of 3CR radio galaxies is truly correlated with both the total radio power and the optical luminosity.

We can also confirm the radio core/total radio correlation for FR 2 galaxies, by extending the sample below the $m = 18$ limit, but only including sources known to be at redshift $z < 0.2$. To define this new sample we used the revised 178 MHz sample of LRL. This sample should be complete to $z = 0.2$, since most of the objects brighter than $m = 19$ have measured redshifts. There are six extra sources in the enlarged sample (3CR 33.1, 3CR 61.1, DA 240, 4C 73.08, 3CR 319, and 3CR 401). The correlation is still present. A Spearman rank test with the worst ranking for the upper limits gives a probability of chance correlation of $\sim 1\%$.

b) l_x versus l_{RN}, l_{RT}, and l_o

Figure 5 shows the plots of l_x versus l_{RT} and l_o for the whole sample and for the FR 1 and FR 2 subsamples. An inspection

TABLE 5

PARTIAL SR CORRELATION COEFFICIENT AND PROBABILITIES (ONE-TAILED)

Sample	ON.T[b]	P	OT.N[b]	P	NT.O[b]	P
Total	0.61	<0.05%	-0.32[a]	2.5%	0.77	<0.05%
FR 1	0.47	2.5%	-0.11[a]	>10%	0.78	<0.05%
FR 2	0.62	0.25%	-0.15[a]	>10%	0.60	0.25%

[a] Anticorrelation.
[b] Partial correlation coefficients (see text).

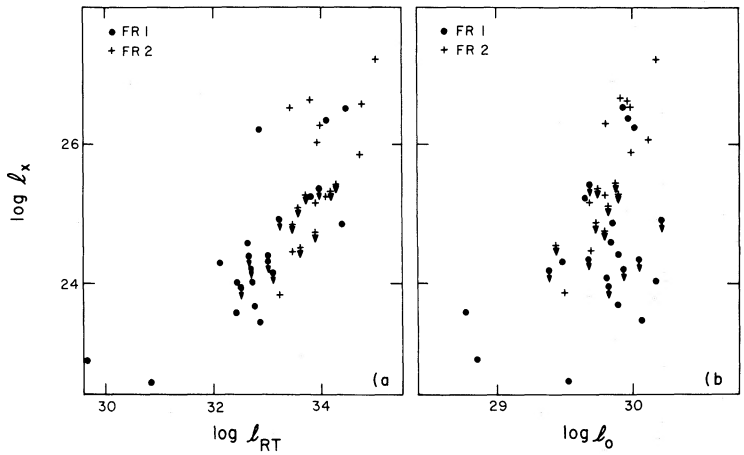

FIG. 5.—(*a*) The logarithm of the monochromatic X-ray luminosity at 2 keV l_x is plotted vs. log l_{RT}; (*b*) log l_x vs. log l_o

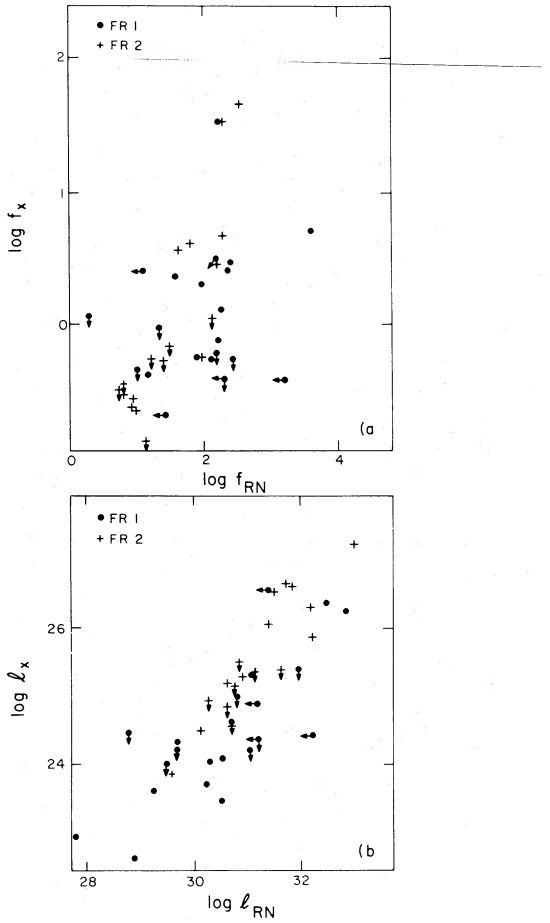

FIG. 6.—(*a*) Log f_x vs. log f_{RN}; (*b*) l_x vs. log l_{RN}

of these plots suggests possible correlations between l_x and l_{RT} and between l_x and l_o. Figure 6 shows the plots of l_x versus l_{RN} and f_x versus f_{RN}. In this instance there is a clear correlation between the luminosities and also between the fluxes for both the total sample and the FR 2 subsample. To quantify these results we used two different and independent methods. First, we used a *worst case* nonparametric approach, by using the Spearman rank (one-sided) test and ranking the upper limits to get the smallest correlation coefficients. Secondly, we applied a parametric method based on the "detections and bounds" technique of Avni (1982) to each correlation. In this way, under the assumption of a linear correlation and of a Gaussian spread of l_x (or f_x), we can determine the significance of the correlation using *all* the information available, including upper limits (for a previous application of this method, see Fabbiano, Feigelson, and Zamorani 1982).

The probabilities from the worst case Spearman rank test (P_{SR}) for the correlations to be due to chance are given in Table 6. The slopes of the correlation with the 68% and 90% (in parentheses) statistical errors from the "detections and bounds" method are also given. The P_{SR}, which are in fact upper limits to the probability of chance correlation, indicate a possible correlation between l_x and l_{RT} for the total sample, and l_x and l_o for the total sample and the FR 2 subsample. The "detections and bounds" method indicates correlations between l_x and l_{RT} for the total sample and the FR 1 subsample, and between l_x and l_o in the total sample. No corresponding correlations between fluxes were observed for the above variables.

Small P_{SR} are obtained for the correlations of l_x with l_{RN} (and f_x with f_{RN}) for both the total sample and the FR 2 subsample. The "detection and bounds" method indicates correlations in all cases.

Since l_x is not *a priori* correlated with the redshift z and since in our analysis we use both detections and upper limits, the correlations that we observe (even if only in luminosity) should not suffer from selection effects. Although we cannot use the Spearman partial rank correlation test to disentangle the dependences of the variables from each other because of the large number of upper limits, we can infer some of these dependences from the results of the previous section. The strongest correlation (seen both in flux and luminosity) is certainly the one between X-ray and nuclear radio emission. Given the correlations between l_{RN} and both l_o, and l_{RT} (see § VI*a*), it is possible that the other correlations could be carried over through l_{RN}.

c) f_x/f_o versus Colors

Although the $U-B$ color was only available for 16 galaxies, there is an indication that galaxies with larger f_x/f_o ratios tend to have an ultraviolet excess. This trend is probably not affected by selection effects, and it most likely indicates stronger nonthermal continuum in the optical spectra of the radio galaxies that are stronger X-ray emitters. These galaxies are also those with broad emission-line spectra.

TABLE 6

SR CORRELATION PROBABILITIES (ONE-TAILED) AND LINEAR FIT SLOPES FOR X-RAY, RADIO, AND OPTICAL CORRELATIONS

	TOTAL		FR 1		FR 2	
$y \propto x$	P_{SR}[a]	Slope[b]	P_{SR}[a]	Slope[b]	P_{SR}[a]	Slope[b]
$l_x \propto l_{RT}$	7%	0.82 ± 0.18 (0.23)	≥5%	0.72 ± 0.15 (0.30)	≥5%	1.4 ± 0.5 (0.9)
$l_x \propto l_o$	7%	2.2 ± 0.4 (1.2)	≥5%	1.15 ± 0.60 (...)	<3%	...
$l_x \propto l_{RN}$	1%	0.97 ± 0.18 (0.20)	≥5%	0.77 ± 0.18 (0.20)	1%	1.05 ± 0.15 (0.25)
$f_x \propto f_{RN}$	<0.1%	0.80 ± 0.08 (0.28)	3%	0.75 ± 0.08 (0.30)	3%	1.22 ± 0.10 (0.38)

[a] With the worst case ranking for the upper limits.

[b] With the detections and bounds method. The value in parentheses is the uncertainty at the 90% confidence level. Ellipsis dots indicate insignificant results.

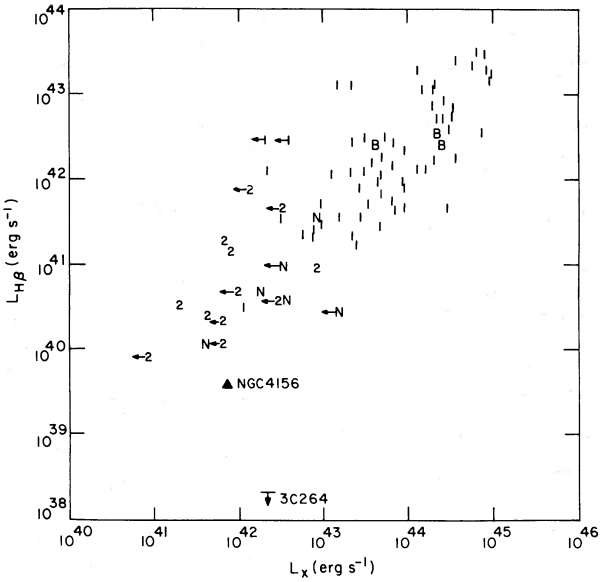

FIG. 7.—Hβ vs. X-ray luminosity (after Kriss and Canizares 1982). The "1" and "2" identify Seyfert type 1 and 2 galaxies. "B" and "N" are broad line and narrow line 3CR galaxies. NGC 4156 and 3C 264 are the two "X-ray bright but optically dull" galaxies from Elvis *et al.* (1981). 3C 264 is also a member of the sample discussed in this paper.

d) L_x *versus Optical Line Luminosities*

Figures 7 and 8 show the plots of $L_{H\beta}$ versus L_x and of $L_{[O\,III]}/L_{H\beta}$ versus L_x for all the galaxies for which the line intensities were available. The line luminosities come from the compilation of Steiner (1981), Yee and Oke (1978), Yee (1980), and Costero and Osterbrock (1977). In Figure 7 we also plot the points from Kriss and Canizares (1982) for type 1 and type 2 Seyfert galaxy detections. In Figure 8 we include the galaxies of Steiner's (1981) classes "B" and "C." These are mainly radio-quiet, weak Fe II emitting, active galaxies, both broad- and narrow-lined. Surprisingly few of the radio galaxies in our sample have *flux-calibrated* optical spectra available in the literature. Some have only photographic spectra. Consequently, we do not have enough optical data to draw any conclusions from the 3CR galaxies alone. We note that they are compatible with the relationships found for radio-quiet (Seyfert) galaxies in the two plots. We discuss this similarity in detail in § VII.

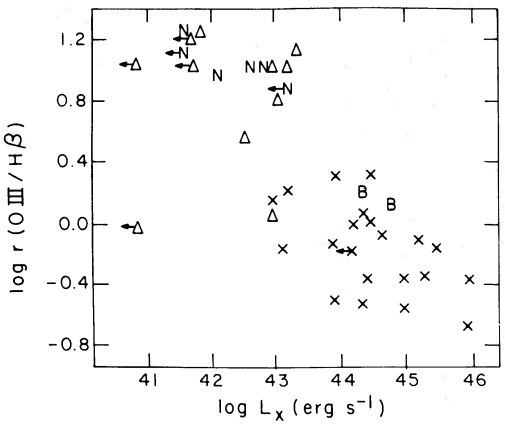

FIG. 8.—The logarithm of the ratio of the O III to Hβ line luminosity is plotted vs. the logarithm of the X-ray luminosity. The crosses are Steiner's (1981) class B objects (broad lines, no Fe II), the triangles are Steiner's class C objects (narrow lines). "B" and "N" are broad line and narrow line 3CR galaxies.

e) L_x *versus Clustering Parameters*

It is difficult to study correlations between the X-ray luminosity of the galaxy L_x and clustering owing to the presence of extended cluster emission, which will contaminate our measurement of the X-ray emission (see § V). This is particularly significant for galaxies at the center of a cluster, and careless handling of the data could result in spuriously high luminosities attributed to the radio galaxies. Our analysis specifically tends to exclude cluster emission.

Correlations between radio power and cluster membership were investigated by Longair and Seldner (1979) and Stocke (1979). We investigated possible relationships between L_x and clustering using both the cross-correlation parameter B_{gg} of Longair and Seldner which measures the number of galaxies per unit volume around a radio source, and the parameter D2 of Stocke, which is more sensitive to small-scale clustering. In both cases no correlations were found for the sample as a whole, indicating that the X-rays from the radio galaxies are not measurably affected by the environment. Those sources which were thought to lie in clusters from the two parameters above were surrounded by large-scale cluster emission, as were other galaxies which lay in regions of enhanced galaxy density: 3CR 310 (Burns, Gregory, and Holman 1981), 3CR 66B (Maccagni and Tarenghi 1981), and 3CR 31.

VII. DISCUSSION

a) *The Correlations*

As discussed in § VI*a*, in the complete radio optical sample of 43 galaxies the nuclear radio luminosities are correlated with both the optical and the total radio luminosity from the radio lobes. A possible correlation between the total and the nuclear radio emission has been explored in the literature (Fanti and Perola 1977; Bridle and Fomalont 1978) but no evidence was found. Feigelson and Berg (1983) find a correlation between l_{RN} and l_{RT} similar to the one discussed in this paper, but using a heterogeneous subsample of 3CR galaxies. There are only five upper limits (which we use) in our complete sample, and moreover we have performed a statistical analysis that considers simultaneously all the possible variables. Therefore, we are confident that the correlations between nuclear radio power and total radio power and between nuclear radio power and optical luminosity are both intrinsically true in the total galaxy sample and in the FR 2 subsample and most likely true also in the FR 1 subsample. The slope (0.75 ± 0.05) that we find for the complete sample correlation between l_{RN} and l_{RT} is steeper than the value (0.5) suggested by Fanti and Perola (1977) using a mixed sample of galaxies. This slope is also identical with that for the FR 1 galaxies (0.75 ± 0.10). However, we find an indication of a steeper slope (1.3 ± 0.3) for the FR 2 galaxies alone. This probably arises from the inclusion in our sample of only optical luminous objects at high redshifts; i.e., the broad-line galaxies. In common with quasars (Miley 1980) these objects tend to have relatively more powerful radio cores. Inspection of FR 2 sources in the LRL

sample indicates a slope of unity for this correlation, when the full variety of optical types are represented.

These correlations point to the importance of nuclear activity in radio galaxies. The correlation between l_{RN} and l_{RT} suggests that the nuclear phenomenon in 3CR galaxies is steady for the lifetime of the source and supports the hypothesis of continuous feeding of the lobes via a beam (Longair, Ryle, and Scheuer 1973; Scheuer 1974). The correlation between l_{RN} and l_o is more difficult to explain. In the FR 2 sample it could be explained at least in part by considering l_o as due to a basic stellar component, present in all 3CR galaxies in a similar amount, plus a nuclear nonthermal component, dominant in the broad-line galaxies (Osterbrock, Koski, and Phillips 1976), but not in the narrow-line galaxies (Costero and Osterbrock 1977). Correlations between the radio luminosity (both total and nuclear) and the nonthermal optical luminosity from the nucleus had been found by Yee and Oke (1978). However, the FR 1 galaxies also show a possible correlation between l_{RN} and l_o, and moreover the optical luminosity is the visual luminosity which in most galaxies is dominated by the stellar component. The data might therefore suggest a relationship between the mass of the galaxy and radio nuclear activity.

Of all the correlations explored in § VI, the strongest is that between l_x and the nuclear radio luminosity at 5 GHz l_{RN}. This correlation points to a nuclear origin for the X-ray emission of at least the FR 2 galaxies. Moreover 3CR 390.3, the only FR 2 galaxy in the sample for which high resolution X-ray data are available, looks pointlike when observed with the HRI. The galaxy 3CR 382 has an upper limit to the X-ray extent smaller than the extent of the radio lobes. We also know that some of the FR 1 galaxies show a pointlike X-ray source coincident with the nucleus (see § IV). However, two very powerful FR 2 radio galaxies, 3C 295 (Henry *et al.* 1979) and Cyg A (Fabbiano *et al.* 1979) are associated with extended X-ray emission, suggesting higher hot gas densities. This and the implications for the problem of confinement will be discussed in Paper II.

Weaker correlations are found between l_x and the total radio power in the lobes at 178 MHz l_{RT} and between l_x and the optical luminosity l_o. Given the observed correlations in the complete radio optical sample, these correlations are likely to be a byproduct of the correlation between l_x and l_{RN}. Significant X-ray emission due to inverse Compton scattering from the radio lobes is excluded at least in those radio sources which have X-ray emission on significantly smaller angular scales (see § IV).

b) *Comparison with Seyfert Galaxy Properties*

The range of L_x and of f_x/f_o (Figs. 1 and 3) for both the sample as a whole and for the two subclasses FR 1 and FR 2 extends to higher X-ray luminosities than those of "normal" elliptical galaxies and overlaps that of Seyfert galaxies. This is particularly true for FR 2 galaxies with the broad-line galaxies at the top of the distribution.

The FR 2 galaxies in our sample show strong emission lines in their optical spectra very similar to those of Seyfert galaxies. As with Seyfert galaxies (Osterbrock 1979; Khachikian and Weedman 1974), these spectra divide roughly into two types: those having broad (5000–10,000 km s^{-1} FWHM) permitted lines and those with only narrow (500–1000 km s^{-1} FWHM) lines, both permitted and forbidden (Grandi and Osterbrock 1978). Given the degree of similarity between the broad-line Seyfert 1 galaxies and broad-line radio galaxies it is natural to ask whether narrow-line radio galaxies are the radio-loud equivalents of type 2 Seyfert galaxies. Our X-ray data allow several new comparisons to be made.

The difference in X-ray luminosities between narrow- and broad-line radio galaxies suggested by our data alone (§ V) is reinforced in two-dimensional plots of X-ray flux or luminosity versus a second, optical, variable such as those in Figures 7 and 8. For the $L_{H\beta}$ versus L_x correlation (Fig. 7), the broad-line galaxies clearly lie with the Seyfert 1 galaxies, as was already known, and the narrow line galaxies lie with the Seyfert 2 galaxies. This strengthens the case (Costero and Osterbrock 1977) that the narrow-line galaxies are photoionized and that the shape of the ionizing continuum is similar in both Seyfert 2 galaxies and narrow-line radio galaxies.

In the plot of [O III]/Hβ versus L_x (Fig. 8), the broad-line galaxies are Steiner's (1981) objects of class "B." They lie in a similar part of the diagram as Seyfert 1 galaxies, which are predominantly Steiner's class "A." The narrow-line radio galaxies again lie with Steiner's (1981) objects of class "C." These comprise of type 2 Seyfert galaxies and X-ray selected Seyfert 1.9 galaxies (i.e., those for which a broad component in visible only on Hα: Osterbrock 1981). These galaxies, which were originally called "narrow emission-line galaxies," are often very dusty and have large low energy X-ray cut-offs (10^{22}–10^{23} atoms cm^{-2}; Maccacaro, Perola, and Elvis 1982 and Mushotzky 1982). If such column densities are present in the narrow-line radio galaxies then their intrinsic X-ray luminosities are underestimated by the IPC by factors of $\sim$10–30. Lawrence and Elvis (1982) have suggested that increased obscuration of the continuum and broad-line region is systematically larger at low intrinsic continuum luminosities at least in radio-quiet active galactic nuclei. In this case the correlation of Figure 8 could be largely the result of this systematic effect. Since the range of l_x for FR 2 galaxies extend over more than three orders of magnitude, this would not affect the correlation with the nuclear radio luminosity l_{RN}, but would only steepen somewhat the slope.

It would be a natural extension of the Lawrence and Elvis (1982) result to suggest that narrow-line radio galaxies are also highly obscured broad-line radio galaxies. There is evidence for this proposition. The Paschen-α observations of 3C 445 by Rudy and Tokunaga (1982) and of 3C 234 by Carleton and Willner (1984) show its flux to be far larger than would be expected based on the Hβ flux and the Hβ/Paα ratios seen in quasars or predicted from recombination theory. Carleton and Willner (1984) have also marginally resolved the line profile showing that the bulk of the Paα emission comes from the broad-line region although broad Hβ is only just detected (Grandi and Phillips 1979).

Other signatures of large obscuration need to be examined, for instance, steep 3.5–10 μm slope, weak broad Hβ, and absorbed low-energy X-ray spectra (Lawrence and Elvis 1982).

c) *Comparison with QSOs*

Since the launch of the *Einstein* satellite a number of papers have been published on the X-ray properties of QSOs (Tananbaum *et al.* 1979; Ku, Helfand, and Lucy 1980; Zamorani *et al.* 1981). More recently Tananbaum *et al.* (1983) have studied the X-ray properties of a complete sample of

33 3CR quasars. Although the X-ray luminosities are typically higher than those of the 3CR radio galaxies, the X-ray to optical flux ratios are similar for QSOs and for the broad emission-line FR 2 galaxies (Figs. 1 and 3). Moreover, the radio morphologies and the optical spectra of FR 2 galaxies and FR 2 quasars are similar. Tananbaum *et al.* (1983) find a relationship between nuclear 5 GHz radio luminosities and the X-ray luminosities of the FR 2 quasars with compact cores which is similar to the relationship found for FR 2 radio galaxies.

There are 18 quasars in Tananbaum *et al.* (1983) with FR 2 morphology; there is one with small-scale double structure (3C 191; Laing 1981*a*); and there are two with double structure around a bright, compact, core (3C 207 and 3C 245; Pooley and Henbest 1974 and Laing 1981*a*). Eleven remaining sources are less than 2″ in size (Ryle and Elsmore 1973; Elsmore and Ryle 1976; Laing 1981*a*), and one has unknown structure on a scale of a few arcseconds (3C 298; Erickson *et al.* 1972). Of the 18 FR 2 quasars, 12 have measured radio cores at either 6 cm or 2 cm, one has the identification coincident with a hot spot (3C 186; Riley and Pooley 1975), and we have set upper limits for the remaining 5 (JPR; Riley and Pooley 1975; Pooley and Henbest 1974; Laing 1981*b* and private communication 1982; Swarup, Sinha, and Saika 1982). Where only 2 cm core flux densities are available we have used those, as they will typically be within a factor of 2 of the 6 cm values. The nuclear radio and the X-ray luminosities of the 17 FR 2 quasars (excluding 3C 186) and the 18 FR 2 radio galaxies from our sample are shown in Figure 9. The quasars follow the relationship between l_x and l_{RN} of the FR 2 galaxies, suggesting a similar mechanism to be active in the two classes of objects. However, if the 3CR galaxies are disregarded, the FR 2 quasars seem to follow a different correlation. With a linear regression we obtain a slope of 0.3 ± 0.13, much flatter than the one derived for radio galaxies (see Table 6). This difference is probably an artifact introduced by the limited statistics and the small luminosity range of the quasars but could also be indicative of absorption in the narrow-line galaxies, as suggested in the previous section, or of a dependence of the X-ray on the optical luminosity of 3CR quasars (Tananbaum *et al.* 1983).

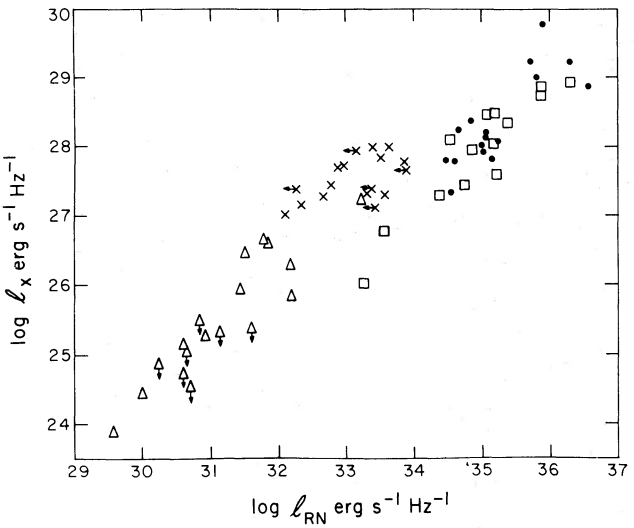

FIG. 9.—Log l_x vs. log l_{RN} for FR 2 galaxies (*triangles*), FR 2 quasars with compact core (*crosses*) (Tananbaum *et al.* 1982), and radio flat quasars (Zamorani *et al.* 1981) (*dots*), and Owen *et al.* (1981) (*squares*).

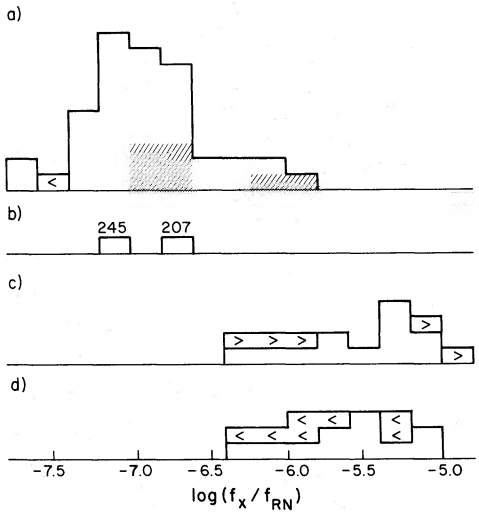

FIG. 10.—Histogram of the log f_x/f_{RN} for (*a*) radio flat quasars, (*b*) "intermediate" quasars (*c*) FR 2 quasars and (*d*) FR 2 galaxies.

In quasars with flat radio spectra, the X-ray luminosity is strongly correlated with radio and millimeter wavelength luminosities, with a slope of about 1 (Owen, Helfand, and Spangler 1981). Also plotted in Figure 9 are those flat-spectrum quasars with measured redshifts from Owen *et al.* and from Zamorani *et al.* (1981). The redshifts and 6 cm flux densities have been taken from Kühr *et al.* (1979) and Kühr *et al.* (1981). The total 6 cm radio fluxes have been used for these objects, as the dominant emission comes from compact regions at this frequency. Thus the compact nuclear regions in all the sources are being compared. Figure 10 shows the histograms of f_x/f_{RN} for FR 2 galaxies, FR 2 quasars, and for the flat-spectrum quasars. The latter have ratios of f_x/f_{RN} which are a factor about 30 lower than in the FR 2 objects. The difference is significant at a level $<0.1\%$ using the one-sided Kolmogorov-Smirnov test, wherever the upper and lower limits are distributed. It is interesting that the two extended sources with bright radio cores (3C 207 and 3C 245) do not have proportionally brighter X-ray emission, and thus have f_x/f_{RN} ratios similar to those in flat-spectrum quasars (see Fig. 10*b*). The radio spectra of these two sources are steep at low frequencies but flat at 6 cm. Hence, these sources appear to be intermediate between FR 2 and flat-spectrum quasars.

There are several possible explanations for these results:

1. The cores in these two types of objects could simply have differing parameters. For example, if the X-ray emission were due to inverse Compton scattering of the radio photons, the brightness temperatures of the cores of the FR 2 objects might be higher than those of the flat radio spectrum quasars.

2. There could be a luminosity dependence of the ratio f_x/f_{RN}. However, this is ruled out by the presence of two flat-spectrum quasars from Owen, Helfand, and Spangler (1981), which have relatively low luminosities, but low f_x/f_{RN} ratios.

3. The objects with relatively bright radio cores (i.e., those with flat high-frequency radio spectra) could have additional radio components of 6 cm which are not associated with the

X-ray emission, and which are either not present in the other cores, or are self-absorbed at 6 cm.

4. Orr and Browne (1982) have suggested that all quasars have cores containing bulk relativistic motion, and that the difference between FR 2 and flat-spectrum quasars is simply the inclination to the line of sight. We can set some limits on this model. If the X-ray emission is unbeamed, then the radio emission can be enhanced by no more than a factor of 30, corresponding to a Lorentz factor ~ 2. This is insufficient to make the cores dominate over the extended structure. The X-ray emission might also be beamed if it arises in the radio-emitting region. However, we believe this is unlikely, as the ratio f_x/f_o covers the same range in flat-spectrum and in FR 2 quasars, and in turn the ratios of optical continuum to line strengths are similar for the few objects with both known radio classification and measured optical spectra (e.g., Yee 1980). Since the emission lines cannot be relativistically beamed, the X-ray emission probably cannot be beamed by the required factor (>10), except possibly in BL Lac–type objects. There could, however, be extra unbeamed radio emission in the cores which would lower the ratio f_x/f_{RN} in the FR 2 objects without requiring beamed X-ray emission. Alternatively, there could be obscuration of both X-ray and optical emission in FR 2 objects, but not in the flat-spectrum objects, if there is obscuration which is a function of the inclination angle. However, the blue optical continua and broad emission lines typical of FR 2 quasars and high l_x radio galaxies (Sandage 1972; Osterbrock, Koski, and Phillips 1976), together with the lack of absorption in the X-ray spectra (Petre *et al.* 1984), argue against absorption in the more X-ray–powerful FR 2 objects. If the obscuration is also a function of l_x as in Seyfert galaxies (Lawrence and Elvis 1982), the FR 2 correlation would still have a flatter slope than that of the flat-spectrum objects. Obscuration alone is not enough to explain these differences.

5. In the Scheuer and Readhead (1979) model, the cores of the FR 2 objects do not have relativistic bulk motion, whereas the cores in flat-spectrum quasars are boosted by relativistic motion in the objects favorably aligned. The unfavorably aligned objects would be radio-quiet QSOs. The difference found between the ratio of f_x/f_{RN} for FR 2 and flat-spectrum quasars does not invalidate this model, even if the relative luminosities of X-ray and radio emission radiated by the cores into 4π steradians are the same in the two classes of objects. The observed difference could be consistent with a Lorentz factor as high as 7, for a flat radio spectrum and continuous ejection of material within the core, as in Scheuer and Readhead. Note, however that there is some evidence that FR 2 objects also contain bulk relativistic motion in their cores (e.g., 3C 111, Hine and Scheuer 1980; 3C 179, Porcas 1981, 1982).

d) The Absorption-Line Galaxies ("optically dull/X-ray bright")

Figure 7 shows the two galaxies reported by Elvis *et al.* (1981). These have very low equivalent widths and fluxes for their emission lines despite having luminous ($\sim 10^{42}$ ergs s^{-1}) nuclear X-ray sources. The narrow-line radio galaxies help us to understand these objects in part. The galaxy NGC 4156 was the radio-quiet example of these "optically dull/X-ray–bright" galaxies. Since it occupies the same region in the $L_{H\beta}$ versus L_x diagram as the narrow-line radio galaxies it is likely that it is merely an extremely low-luminosity Seyfert type 2 galaxy. The radio-loud counterparts to NGC 4156 are easily picked out as active by radio surveys but are not distinguished by their optical spectra alone. If the radio-quiet/radio-loud ratio of occurrence is ~ 10 (Shaffer, Green, and Schmidt 1982; Smith and Wright 1980), then the majority of such objects are missed by present surveys (e.g., Markarian, Lipovetsky, and Stepanian 1981 and references therein; MacAlpine, Lewis, and Smith 1977).

The galaxy 3C 264, the radio-loud "optically dull" galaxy from Elvis *et al.* (1981), is also a member of our complete sample. It clearly falls below the $L_{H\beta}$ versus L_x correlation of Figure 7. However, it does lie on the l_{RN} (5 GHz) versus l_x correlation of Figure 6. This strengthens the case that X-ray emission from FR 1 galaxies is also nuclear. It also implies that it is not the nature of the continuum source itself but rather the conditions around the source, such as absence of gas to be photoionized, that cause the extremely low emission-line strengths in 3C 264 and in FR 1 galaxies in general.

The presence of double radio structures and the predominantly stellar galaxy spectra rules out relativistic bulk motions as an explanation for the weakness of the emission lines for the FR 1 galaxies as a class.

VIII. CONCLUSIONS

The principal results of our X-ray survey of a complete sample of 3CR radio galaxies are the following:

1. Twenty-six of the 40 3CR galaxies observed with *Einstein* were detected (at or above 3 σ) with (0.5–3.0 keV) X-ray luminosities from 1.7×10^{41} to 1.0×10^{45} ergs s^{-1} ($H_0 = 50$ km s^{-1} Mpc^{-1}). The galaxies in clusters are embedded in extended X-ray emission, presumably from the hot cluster medium. Within the resolution of the instrument, the detected isolated galaxies are consistent with a point source.

2. By comparing the distributions of L_x of the 3CR galaxies in either the two radio classes FR 1 and FR 2 (Fanaroff and Riley 1974) or the two optical classes A and B (Hine and Longair 1979), we find a suggestion that FR 2 (class A) galaxies are stronger X-ray emitters than FR 1 (class B) galaxies. The galaxies with broad emission lines in their optical spectra are at the high X-ray luminosity end of the distribution, with L_x values comparable with those of Seyfert 1 galaxies.

3. By analyzing the complete optical and radio sample with the Spearman partial rank correlation technique, we find that the nuclear radio luminosities at 5 GHz are correlated with the total extended radio luminosities at 178 MHz and also with the optical luminosities.

4. The X-ray luminosity is strongly correlated with the nuclear radio luminosity at 5 GHz. The correlation is stronger for FR 2 than FR 1 galaxies, which present a larger scatter. Other less strong correlations are present between the X-ray luminosity and both the total radio luminosity at 178 MHz and the optical luminosity.

These results point to the importance of nuclear activity in radio galaxies. The correlation between nuclear and extended radio power indicates that the nuclear phenomenon is steady for the lifetime of the source and supports the hypothesis of continuous feeding of the lobes. The correlation between nuclear radio power and optical luminosity suggests that nuclear activity is more likely in more luminous (i.e., more

massive) galaxies or stronger optical nuclei. The correlation between X-ray luminosity and nuclear radio power suggests a nuclear origin for the X-ray emission. Our data, however, cannot be used to constrain different possible mechanisms, like synchrotron self-Compton (Jones, O'Dell, and Stein 1974) or direct synchrotron emission from the nucleus. Constraints can be put on the amount of hot gas that could confine the radio lobes. This issue will be explored in a following paper.

The 3CR emission-line galaxies are similar to both Seyfert galaxies and extended 3CR quasars in their X-ray properties, strongly reinforcing a unified picture of active nuclei. Similarities with Seyfert galaxies suggest that the narrow-line radio galaxies have highly obscured nuclei suppressing the broad lines and the continuum. Compact quasars, however, show significant differences in their X-ray/radio properties.

The non–emission-line radio galaxies also probably contain nuclear X-ray sources. This suggests that absence of emission lines in these galaxies is not due to the absence of an ionizing continuum but rather to the absence of cool clouds of gas around the nucleus.

These results call for several specific observing programs to be undertaken. Most obvious is the lack of flux-calibrated optical spectra. Far infrared photometry or infrared line spectra (e.g., Paα will be needed to test the hypothesis of obscuration. These programs are possible with present facilities. The proposed Advanced X-Ray Astrophysics Facility will allow us not only to resolve the radio galaxies within the clusters but also to make detailed study of the X-ray spectra.

We thank all our colleagues who made this study possible by allowing us to use X-ray fluxes from unpublished observations of 3CR galaxies. In particular, we thank Eric Feigelson, Loretta Gregorini, Christine Jones, Dan Harris, David Helfand, Ethan Schreier, Joseph Silk, and Tony Tyson. We thank Robert Laing, Patrick Leahy, Guy Pooley, and Dave Stannard for providing radio core flux densities before publication.

We acknowledge useful discussions with Yoram Avni, Eric Feigelson, and Gianni Zamorani. We thank Harvey Tananbaum for a critical reading of the manuscript and Paolo Giommi for the use of his plotting routines. This work was supported in part by NASA contract NAS8-30751. L. M. acknowledges financial support from the SERC and the Cavendish Laboratory. G. T. acknowledges financial support from the Italian CNR. M. L. was an *Einstein Observatory* Guest Observer.

REFERENCES

Argue, A. N., Riley, J. M., and Pooley, G. G. 1978, *Observatory*, **98**, 132.
Avni, Y. 1984, in preparation.
Avni, Y., Soltan, A., Tananbaum, H., and Zamorani, G. 1980, *Ap. J.*, **238**, 800.
Baldwin, J. E. 1982, in *IAU Symposium 97, Extragalactic Radio Sources*, ed. D. S. Heeschen and C. M. Wade (Dordrecht: Reidel), p. 21.
Branduardi-Raymont, G., Fabricant, D., Feigelson, E., Gorenstein, P., Grindlay, J., Soltan, A., and Zamorani, G. 1981, *Ap. J.*, **248**, 55.
Bridle, A. H., and Fomalont, E. B. 1978, *A.J.*, **83**, 704.
Bridle, A. H., Fomalont, E. B., and Cornwell, T. J. 1981*b*, *A.J.*, **86**, 1294.
Bridle, A. H., Fomalont, E. B., Palimaka, J. J., and Willis, A. G. 1981*a*, *Ap. J.*, **248**, 499.
Bridle, A. H., and Vallée, J. P. 1981, *A.J.*, **86**, 1165.
Burns, J. O., and Christiansen, W. A. 1980, *Nature*, **287**, 208.
Burns, J. O., Gregory, S. A., and Holman, G. D. 1981, *Ap. J.*, **250**, 450.
Carleton, N., and Willner, S. 1984, in preparation.
Costero, R., and Osterbrock, D. E. 1977, *Ap. J.*, **211**, 675.
Elsmore, B., and Ryle, M. 1976, *M.N.R.A.S.*, **174**, 411.
Elvis, M., Schreier, E. J., Tonry, J., Davis, M., and Huchra, J. P. 1981, *Ap. J.*, **246**, 20.
Erickson, W. C., Kuiper, T. B. H., Clark, T. A., Krowles, S. H., and Broderick, J. J. 1972, *Ap. J.*, **177**, 101.
Fabbiano, G., Doxsey, R. E., Johnston, M. D., Schwartz, D. A., and Schwarz, J. 1979, *Ap. J.* (*Letters*), **230**, L67.
Fabbiano, G., Feigelson, E., and Zamorani, G. 1982, *Ap. J.*, **256**, 397.
Fabian, A. C. 1979, *Proc. Roy. Soc. London, A*, **366**, 449.
Fabricant, D., Branduardi, G., Gorenstein, P., and Zamorani, G. 1979, *Bull. AAS*, **4**, 784.
Fanaroff, B. L., and Riley, J. M. 1974, *M.N.R.A.S.*, **167**, 31P.
Fanti, R., and Perola, C. C. 1977, in *IAU Symposium 74, Radio Astronomy and Cosmology*, ed. D. L. Jauncey (Dordrecht: Reidel), p. 171.
Feigelson, E., and Berg, C. 1983, *Ap. J.*, **269**, 400.
Fomalont, E. B., and Bridle, A. H. 1978, *A.J.*, **83**, 725.
Fomalont, E. B., Palimaka, J. J., and Bridle, A. H. 1981, *A.J.*, **85**, 981.
Fomalont, E. B., Bridle, A. H., and Miley, G. K. 1982, *IAU Symposium 97, Extragalactic Radio Sources*, ed. D. S. Heeschen and C. M. Wade (Dordrecht: Reidel), p. 173.
Forman, W., Schwarz, J., Jones, C., Liller, W., and Fabian, A. C. 1979, *Ap. J.* (*Letters*), **234**, L27.
Forman, W., and Jones, C. 1982, *Ann. Rev. Astr. Ap.*, **20**, 547.
Giacconi, R., *et al.* 1979, *Ap. J.*, **230**, 540.
Grandi, S. A., and Osterbrock, D. E. 1978, *Ap. J.*, **220**, 783.
Grandi, S. A., and Phillips, M. M. 1979, *Ap. J.*, **232**, 659.
Gregorini, L., *et al.* 1983, in preparation.
Guthrie, B. N. G. 1981, *M.N.R.A.S.*, **194**, 261.
Hargrave, P. J. 1974, *M.N.R.A.S.*, **168**, 491.
Hargrave, P. J., and McEllin, M. 1975, *M.N.R.A.S.*, **173**, 37.
Harris, D. H., and Grindlay, J. E. 1979, *M.N.R.A.S.*, **188**, 25.
Heckman, T. M., Miley, G. K., Balick, B., van Breugel, W., and Butcher, H. R. 1982, *Ap. J.*, **262**, 529.
Heiles, C. 1975, *Astr. Ap. Suppl.*, **20**, 37.
Henry, J. P., Branduardi, G., Briel, U., Fabricant, D., Feigelson, E., Murray, S., Soltan, A., and Tananbaum, H. 1979, *Ap. J.* (*Letters*), **234**, L15.
Hine, R. G., and Longair, M. S. 1979, *M.N.R.A.S.*, **188**, 111.
Hine, R. G., and Scheuer, P. A. G. 1980, *M.N.R.A.S.*, **193**, 285.
Högbom, J. A. 1979, *Astr. Ap. Suppl.*, **36**, 173.
Jenkins, C. J., Pooley, G. G., and Riley, J. M. 1977, *Mem. R.A.S.*, **84**, 61 (JPR).
Jones, T. W., O'Dell, S. L., and Stein, W. A. 1974, *Ap. J.*, **188**, 353.
Kellerman, K. I., Pauliny-Toth, I. I. K., and Williams, P. J. S. 1969, *Ap. J.*, **157**, 1.
Kendall, M., and Stuart, A. 1976, *The Advanced Theory of Statistics*, Vol. **2** (3rd ed.; London: Charles Griffin and Co.).
Khachikian, E. Ye, and Weedman, D. W. 1974, *Ap. J.*, **192**, 581.
Kriss, G. A., and Canizares, C. R. 1982, *Ap. J.*, **261**, 51.
Kriss, G. A., Canizares, C. R., and Ricker, G. R. 1980, *Ap. J.*, **242**, 492.
Ku, W. H.-M., Helfand, D. J., and Lucy, L. B. 1980, *Nature*, **288**, 323.
Kühr, H., Nauber, U., Pauliny-Toth, I. I. K., and Witzel, A. 1979, *Astr. Ap. Suppl.*, **45**, 367.
Kühr, H., Witzel, A., Pauliny-Toth, I. I. K., and Nauber, U. 1981, Max-Planck Institute für Radioastronomie, Bonn, preprint No. 55.
Laing, R. A. 1981*a*, *M.N.R.A.S.*, **194**, 301.
———. 1981*b*, *M.N.R.A.S.*, **195**, 261.
Laing, R. A., Riley, J. M., and Longair, M. S. 1983, *M.N.R.A.S.*, **204**, 151 (LRL).
Lawrence, A., and Elvis, M. 1982, *Ap. J.*, **256**, 410.
Long, K. S., and Van Speybroeck, L. P. 1982, in *Accretion Driven Stellar X-ray Sources*, ed. W. Lewin and E. van den Heuvel, in press.
Longair, M. S., Ryle, M., and Scheuer, P. A. G. 1973, *M.N.R.A.S.*, **164**, 243.
Longair, M. S., and Seldner, M. 1979, *M.N.R.A.S.*, **189**, 433.
Maccacaro, T., Perola, G. C., and Elvis, M. 1982, *Ap. J.*, **257**, 47.
Maccagni, D., and Tarenghi, M. 1981, *Ap. J.*, **243**, 42.
Macklin, J. T. 1982, *M.N.R.A.S.*, **199**, 1119.
———. 1983, *M.N.R.A.S.*, **203**, 147.
MacAlpine, G. M., Lewis, D. W., and Smith, S. B. 1977, *Ap. J. Suppl.*, **35**, 203.
Marshall, F. E., Mushotzky, R. F., Boldt, E. A., Holt, S. S., Rothschild, R. E., and Serlemitsos, P. J. 1978, *Nature*, **275**, 624.
Markarian, R. E., Lipovetzky, V. A., and Stepanian, J. A. 1981, *Astrofizika*, **17**, 619.
McKee, J. D., Mushotzky, R. F., Boldt, E. A., Holt, S. S., Marshall, F. E., Pravdo, S. H., and Serlemitsos, P. J. 1980, *Ap. J.*, **242**, 843.
Miley, G. K. 1980, *Ann. Rev. Astr. Ap.*, **18**, 165.
Miley, G. K., and Osterbrock, D. E. 1979, *Pub. A.S.P.*, **91**, 257.
Miley, G. K., Norman, C., Silk, J., and Fabbiano, G. 1983, *Astr. Ap.*, **122**, 330.
Miller, L., and Laing, R. A. 1983, in preparation.
Miller, L., Longair, M. S., Fabbiano, G., Trinchieri, G., and Elvis, M. 1984, in preparation (Paper II).

Mushotzky, R. 1982, *Ap. J.*, **256**, 92.
Orr, M. J. L., and Browne, I. W. A. 1982, *M.N.R.A.S.*, **200**, 1067.
Osterbrock, D. 1979, *A.J.*, **84**, 901.
———. 1981, *Ap. J.*, **249**, 462.
Osterbrock, D., Koski, A. T., and Phillips, M. M. 1976, *Ap. J.*, **206**, 898.
Owen, F. N., Burns, J. P., and Rudnick, L. 1978, *Ap. J.* (*Letters*), **226**, L119.
Owen, F. N., Helfand, D. J., and Spangler, S. R. 1981, *Ap. J.* (*Letters*), **250**, L55.
Pearson, T. J., and Readhead, A. C. S. 1981, *Ap. J.*, **248**, 61.
Perley, R. A., Bridle, A. H., Willis, A. G., and Fomalont, E. B. 1980, *A.J.*, **85**, 499.
Perley, R. A., Willis, A. G., and Scott, J. S. 1979, *Nature*, **281**, 437.
Petre, R., Mushotzky, R., Krolik, J., and Holt, S. 1984, *Ap. J.*, submitted.
Pooley, G. G., and Henbest, S. N. 1974, *M.N.R.A.S.*, **169**, 477.
Porcas, R. W. 1981, *Nature*, **294**, 47.
———. 1982, in *IAU Symposium 97, Extragalactic Radio Sources*, ed. D. S. Heeschen and C. M. Wade (Dordrecht: Reidel), p. 361.
Preuss, E., Pauliny-Toth, I. I. K., Witzel, A., Kellerman, K. I., and Shaffer, D. B. 1977, *Astr. Ap.*, **54**, 297.
Riley, J. M., and Pooley, G. G. 1975, *Mem. R.A.S.*, **80**, 105.
Rudy, R. J., and Tokunaga, A. T. 1982, *Ap. J.* (*Letters*), **256**, L1.
Ryle, M., and Elsmore, B. 1973, *M.N.R.A.S.*, **164**, 223.
Sandage, A. 1972, *Ap. J.*, **178**, 25.
Scheuer, P. A. G. 1974, *M.N.R.A.S.*, **166**, 513.
Scheuer, P. A. G., and Readhead, A. C. S. 1979, *Nature*, **277**, 182.
Schilizzi, R. T. 1976, *A.J.*, **81**, 946.
Schreier, E. J., Gorenstein, P., and Feigelson, E. D. 1982, *Ap. J.*, **261**, 42.
Schwarz, J., *et al.* 1979, *Ap. J.* (*Letters*), **231**, L105.
Shaffer, D. B., Green, R. F., and Schmidt, M. 1982, in *IAU Symposium 97, Extragalactic Radio Sources*, ed. D. S. Heeschen and C. M. Wade (Dordrecht: Reidel), p. 367.
Siegel, S. 1956, *Non-Parametric Statistics for the Behavioral Sciences* (New York: McGraw-Hill).
Smith, H. E., and Spinrad, H. 1980, *Pub. A.S.P.*, **92**, 553.
Smith, H. E., Spinrad, H., and Smith, E. O. 1976, *Pub. A.S.P.*, **88**, 621.
Smith, M. G., and Wright, A. E. 1980, *M.N.R.A.S.*, **191**, 871.
Steiner, J. E. 1981, *Ap. J.*, **250**, 469.
Stocke, J. 1979, *Ap. J.*, **230**, 40.
Strom, R. G., Willis, A. G., and Wilson, A. S. 1978, *Astr. Ap.*, **68**, 367.
Swarup, G., Sinha, R. P., and Saikia, D. J. 1982, *M.N.R.A.S.*, **201**, 393.
Tananbaum, H., *et al.* 1979, *Ap. J.* (*Letters*), **234**, L9.
Tananbaum, H., Wardle, J. F. C., Zamorani, G., and Avni, Y. 1983, *Ap. J.*, **268**, 60.
Turland, B. D. 1975, *M.N.R.A.S.*, **170**, 281.
van Breugel, W. 1980*a*, Ph.D. thesis, Sterrewacht, Leiden.
———. 1980*b*, *Astr. Ap.*, **81**, 265.
Watson, M. G., and Griffiths, R. E. 1984, *Ap. J.*, submitted.
Willis, A. G., and Strom, R. G. 1978, *Astr. Ap.*, **62**, 375.
Yee, H. K. C. 1980, *Ap. J.*, **241**, 894.
Yee, H. K. C., and Oke, J. B. 1978, *Ap. J.*, **226**, 753.
Zamorani, G., *et al.* 1981, *Ap. J.*, **245**, 357.

M. Elvis, G. Fabbiano, and G. Trinchieri: Harvard-Smithsonian Center for Astrophysics, 60 Garden Street, Cambridge, MA 02138

M. Longair: Royal Observatory, Blackford Hill, Edinburgh, Scotland, UK

L. Miller: Department of Astronomy, Royal Observatory, Blackford Hill, Edinburgh, Scotland, UK